Biophysical Journal Volume 73 July 1997 428–445

Compartmentalized Energy Transfer in Cardiomyocytes: Use of Mathematical Modeling for Analysis of In Vivo Regulation of Respiration

Mayis K. Aliev* and Valdur A. Saks#§

*Laboratory of Experimental Cardiac Pathology, Cardiology Research Center, Moscow, Russia; #Laboratories of Bioenergetics, Joseph Fourier University, Grenoble, France; and §Institute of Chemical and Biological Physics, Tallinn, Estonia

ABSTRACT The mathematical model of the compartmentalized energy transfer system in cardiac myocytes presented includes mitochondrial synthesis of ATP by ATP synthase, phosphocreatine production in the coupled mitochondrial creatine kinase reaction, the myofibrillar and cytoplasmic creatine kinase reactions, ATP utilization by actomyosin ATPase during the contraction cycle, and diffusional exchange of metabolites between different compartments. The model was used to calculate the changes in metabolite profiles during the cardiac cycle, metabolite and energy fluxes in different cellular compartments at high workload (corresponding to the rate of oxygen consumption of 46 μ atoms of O · (g wet mass)$^{-1}$ · min^{-1}) under varying conditions of restricted ADP diffusion across mitochondrial outer membrane and creatine kinase isoenzyme "switch-off." In the complete system, restricted diffusion of ADP across the outer mitochondrial membrane stabilizes phosphocreatine production in cardiac mitochondria and increases the role of the phosphocreatine shuttle in energy transport and respiration regulation. Selective inhibition of myoplasmic or mitochondrial creatine kinase (modeling the experiments with transgenic animals) results in "takeover" of their function by another, active creatine kinase isoenzyme. This mathematical modeling also shows that assumption of the creatine kinase equilibrium in the cell may only be a very rough approximation to the reality at increased workload. The mathematical model developed can be used as a basis for further quantitative analyses of energy fluxes in the cell and their regulation, particularly by adding modules for adenylate kinase, the glycolytic system, and other reactions of energy metabolism of the cell.

INTRODUCTION

Recent extensive experimental research in cell biology and biochemistry of coupled creatine kinases, including transgenic animal studies as well as metabolic studies of the isolated heart at different workloads, have led to the understanding that energy metabolism of muscle cells cannot be described as an ideal, homogeneous system of enzymatic reactions (Wallimann et al., 1992; Koretsky, 1995; Wan et al., 1993; Balaban, 1990; Saks and Ventura-Clapier, 1994; Saks et al., 1995, 1996). For example, it has been directly demonstrated that a simple Michaelis-Menten type of relationship does not explain cellular regulation of respiration by cytoplasmic ADP in the heart (Wan et al., 1993). This means that for a quantitative description of metabolic systems in vivo, knowledge of the kinetics of isolated enzymes is not sufficient, and complex intracellular interactions should be accounted for (Saks and Ventura-Clapier, 1994; Saks et al., 1995, 1996).

It is therefore necessary to develop new methods for the quantitative description of compartmentalized energy metabolism in the cells in vivo. With this purpose in mind, we have recently constructed mathematical models of aerobic energy production in heart mitochondria and its control by the coupled creatine kinase reaction (Aliev and Saks, 1993, 1994). In this work we present a more complete mathematical model of intracellular energy supply in cardiac cells that is based on experimentally determined parameters and includes, in addition to a simplified (in comparison to the probability approach) mathematical description of coupled reactions of aerobic phosphocreatine production in mitochondria, descriptions of metabolic and energy fluxes in cytoplasm, and coupled biochemical reactions of energy utilization in myofibrils. This model also includes the description of a new phenomenon: changes in the permeability of mitochondrial outer membrane for adenine nucleotides recently revealed in experiments with permeabilized cardiomyocytes and skinned cardiac fibers (Saks et al., 1995, 1996). The compartmentalized metabolic fluxes across the mitochondrial membranes and in myofibrils, and changes in metabolite levels within one cardiac cycle were calculated. The results of these calculations are helpful in the interpretation of several groups of recent experimental data, including those with transgenic mice with "knocked-out" MM or mitochondrial creatine kinase (Koretsky, 1995; van Deursen et al., 1993, 1994a,b). Analysis of the model shows that 1) restriction of movement of adenine nucleotides across the outer mitochondrial membrane stabilizes the functioning of the coupled mitochondrial creatine kinase-oxidative phosphorylation system, increasing the role of the creatine-phosphocreatine system in energy transfer between subcellular compartments and in the metabolic regulation of respiration; 2) increased permeability of mitochondrial outer membrane for adenine nucleotides in energy-deficient states or after "knock-out" of myoplasmic creatine kinase allows rapid rephosphorylation of cytoplasmic ADP by

Received for publication 21 October 1996 and in final form 24 March 1997.

Address reprint requests to Dr. M. K. Aliev, Cardiology Research Center, 3rd Cherepkovskaya Str., 15A, 121552 Moscow, Russia. Fax: 7-095-414-66-99.

0006-3495/97/07/428/18 $2.00

mitochondrial creatine kinase. Under these conditions mitochondrial creatine kinase catalyzes both phosphocreatine production and its utilization during different phases of the cardiac cycle. Symmetrically, this is also true for the case in which mitochondrial creatine kinase gene is inactive: in this case increased permeability of the mitochondrial outer membrane for adenine nucleotides allows myoplasmic creatine kinase to carry out both synthesis and utilization of phosphocreatine in different phases of the contraction cycle. It was also found that most of the time in the contraction cycle, the creatine kinase reactions are in different steady states, far from equilibrium.

METHODS

General description of the model

Fig. 1 shows the general scheme of the compartmentalized energy exchange between mitochondrial and myofibrillar compartments. This scheme is based on much experimental evidence extensively reviewed in Wallimann et al. (1992), Koretsky (1995), Saks and Ventura-Clapier (1994), and Saks et al. (1995, 1996).

The differential equations for plane diffusion of ATP, ADP, creatine (Cr), phosphocreatine (PCr), and P_i along the chosen diffusion path were solved numerically (Crank, 1975) with diffusion constants for myoplasm taken from Meyer et al. (1984). The computations on the basis of Runge-Kutta-Nistrom algorithm (Ebert and Ederer, 1985) gave the metabolite concentrations for every 13th segment of the diffusion path at each 0.01-ms time step. In mitochondria, ATP is synthesized in the matrix by ATP synthase, and after translocation across the inner mitochondrial membrane it is used for phosphocreatine synthesis in the coupled mitochondrial creatine kinase reaction; in myofibrils creatine kinase (EC 2.7.3.2) is considered to be distributed homogeneously inside the myofibrillar compartment. The calculated concentrations of substrates along the diffusion pathway have been used for calculations of enzymatic rates at each segment of space and time to take into account the concentration changes due to enzymatic activities. Functional coupling of mitochondrial isoenzyme of creatine kinase (CK_{mit}) to adenine nucleotide translocase was modeled by means of high local ATP in a 10-nm narrow space (microcompartment) between coupled molecules. ATP concentration in this microcompartment rises because of a $\sim 10^6$-fold local retardation of ATP diffusion. The values of the coefficients of the diffusion restriction from this local compartment were estimated from the deviation of the mass action ratio of CK_{mit} from the creatine kinase equilibrium constant value observed experimentally (Saks et al., 1985; Soboll et al., 1992, 1994) in coupled rat heart mitochondria under conditions of oxidative phosphorylation.

During contraction, the myofibrils were supposed to hydrolyze ATP with kinetics predicted from the dP/dt change in isovolumic rat hearts: a linear increase in the ATP hydrolysis rate up to 30 ms, followed by its linear decrease to zero at 60 ms at a heart rate of 333 beats · min^{-1}. The total amount of hydrolyzed ATP was taken to be 0.414 mmol · (kg wet mass)$^{-1}$ in one cardiac contraction cycle. This corresponds to an oxygen consumption rate of 23 mmol · (kg wet mass)$^{-1}$ · min^{-1} at a heart rate of 333 beats · min^{-1}.

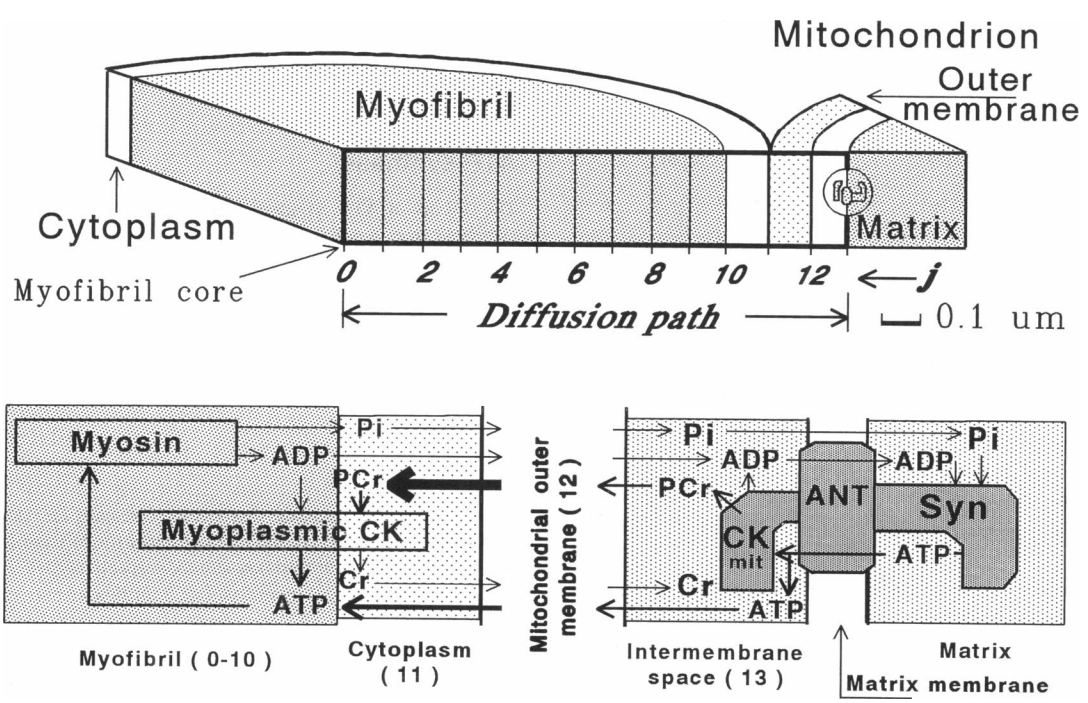

FIGURE 1 The general scheme of compartmentalized energy transfer in cardiac cell. In the model the diffusional exchange of ATP, ADP, PCr, Cr, and P_i between myofibrils and mitochondria is considered along their radii. Interposed among them is a layer of cytoplasm. A diffusion path of 1.3 μm includes 10 0.1-μm space units in myofibril and three units in cytoplasm, mitochondrial outer membrane, and intermembrane compartments. The lower part of the figure shows compartmentalization of myoplasmic CK in myofibril and cytoplasm spaces, of mitochondrial CK (CK_{mit}) and adenine nucleotide translocase (ANT) in the mitochondrial intermembrane space, and of mitochondrial ATP synthase (Syn) in the mitochondrial matrix space. Myofibrillar myosin provides ATP hydrolysis during myofibril contraction. CK_{mit} and ANT are proposed to be coupled by high local ATP concentration, arising from restricted ATP diffusion in the narrow gap (microcompartment) between coupled molecules. Arrows indicate diffusion fluxes of metabolites in compartments and between them through the mitochondrial outer membrane.

The main equations

Diffusion between myofibrils and mitochondria

The plane diffusion of metabolites along the chosen diffusion path (Fig. 1) was calculated numerically by the explicit finite-difference method (Crank, 1975), using the Runge-Kutta-Nistrom algorithm (Ebert and Ederer, 1985). The basic equation of this method predicts a metabolite concentration C for the next time point ($t + \Delta t$) from the known values of metabolite concentrations at a given time t:

$$C_j^{t+\Delta t} = C_j^t + r \times (C_{j-1}^t - 2 \times C_j^t + C_{j+1}^t) \quad (1)$$

In this equation C denotes concentration; t and ($t + \Delta t$) superscripts indicate the time position of C; $j - 1$, j, and $j + 1$ subscripts indicate the space position of C at j variation from zero to 13 (Fig. 1); the diffusion constant r is equal to $D_x \times \Delta t/\Delta l^2$; D_x is the diffusion coefficient for an x sort of metabolite; Δt is the time increment; Δl is the distance between two adjacent points in the diffusion path (Fig. 1).

The method is designed for calculations in cases with fixed metabolite concentrations at both boundaries of a plane sheet (Ebert and Ederer, 1985). To avoid this inconvenience, the myofibril was treated as a symmetrical system (Fig. 2 *A*), with maximum (or minimum) concentrations in the myofibril core ($j = 0$; Figs. 1 and 2 *A*). In such a system C_1^t is equal to C_{-1}^t (Fig. 2 *A*), so $C_0^{t+\Delta t}$ in Eq. 1 is determined by changing the values of C_0^t and $C_1^t = C_{-1}^t$:

$$C_0^{t+\Delta t} = C_0^t + r \times 2 \times (C_1^t - C_0^t) \quad (1a)$$

At the other boundary ($j = 13$, Fig. 1) diffusion stops at the mitochondrial inner membrane. This case can be modeled by taking the real C_{13}^t equal to assumed additional C_{14}^t:

$$C_{13}^{t+\Delta t} = C_{13}^t + r \times (C_{12}^t - C_{13}^t) \quad (1b)$$

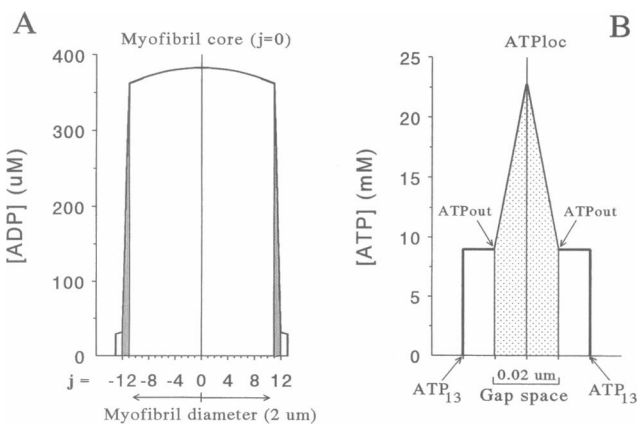

FIGURE 2 Symmetry in space profiles of metabolite concentrations in the whole myofibril with adjoined diffusion spaces (*A*) or in the intermolecular gap between coupled CK_{mit} and ANT complexes (*B*). The data shown are from the 40th millisecond of the cardiac cycle. The simulation was carried out for a complete system with restricted adenine nucleotide diffusion through mitochondrial outer membrane at $res_{ATP} = res_{ADP} = 0.007$. Because of symmetry, the metabolite concentrations are equal at opposing space pairs, $j = 1$ and $j = -1$, $j = 4$ and $j = -4$, etc. (*A*), or in ATPout pairs (*B*). The diffusion restrictions on mitochondrial outer membrane (*shaded areas* in *A*) or in the intermolecular gap (*shaded area* in *B*) result in a drastic elevation in metabolite levels in myofibril and cytoplasm (*A*) or in the intermolecular gap (*B*). ATP_{loc}, ATP_{out}, and ATP_{13} in *B* denote ATP levels in the gap, on its outer boundary, and in the bulk of the mitochondrial intermembrane space, respectively.

Restricted diffusion through the mitochondrial outer membrane

Restricted diffusion through the mitochondrial outer membrane was simulated by changing the value of the diffusion constant (r) in the membrane space (the space between $j = 11$ and $j = 12$ in Figs. 1 and 2 *A*). According to equation 8.45 of Crank (1975), the basic Eq. 1 can be rewritten for the concentrations at both faces of the membrane ($C_{11}^{t+\Delta t}$ and $C_{12}^{t+\Delta t}$) as

$$C_{11}^{t+\Delta t} = C_{11}^t + r \times (C_{10}^t - C_{11}^t) - r \times \text{resm} \times (C_{11}^t - C_{12}^t) \quad (1c)$$

$$C_{12}^{t+\Delta t} = C_{12}^t + r \times \text{resm} \times (C_{11}^t - C_{12}^t) - r \times (C_{12}^t - C_{13}^t) \quad (1d)$$

According to these equations, diffusion in the spaces just before (between C_{10}^t and C_{11}^t) and after (between C_{12}^t and C_{13}^t) the membrane occurs with an unchanged diffusion constant (r), whereas in the membrane space (between C_{11}^t and C_{12}^t) it takes place at the changed diffusion constant ($r \times$ resm). resm (resistance of membrane, resm ≤ 1) reflects the degree of decrease of the diffusion coefficient in the membrane space.

Creatine kinase

Activities of mitochondrial creatine kinase (CK_{mit}) and myoplasmic creatine kinases (CK_{myo}), v_{net}^{CKmit}, and v_{net}^{CKmyo}, respectively, were calculated from the steady-state equation 13 of Saks et al. (1975), using the experimentally determined values of kinetic constants (Jacobus and Saks, 1982) and substrate concentrations in each space segment calculated from diffusion equations. For CK_{mit} the ATP concentrations were local ones (see below, simple diffusional coupling between mitochondrial creatine kinase and adenine nucleotide translocase), whereas ADP, Cr, and PCr concentrations were those in the mitochondrial intermembrane space ($j = 13$; Fig. 1).

ATP synthase

The activity of ATP synthase (Syn) (EC 3.6.1.3) in the matrix space was estimated from a simple kinetic scheme:

$$E + ADP \underset{}{\overset{K_d}{\longleftrightarrow}} E \cdot ADP \overset{K_p}{\longleftrightarrow} E \cdot ADP \cdot P_i \underset{k_r}{\overset{k_f}{\longleftrightarrow}} E \cdot ATP \overset{K_a}{\longleftrightarrow} E + ATP$$

where K_d, K_p, and K_a are the dissociation constants for ADP, P_i, and ATP, respectively; k_f and k_r are the rate constants for forward (ATP synthesis) and reverse (ATP hydrolysis) reactions, respectively.

The steady-state activity of Syn (v_{net}^{syn}) for this scheme can be expressed as

$$v_{net}^{syn} = V_f^{max} \times [ADP] \times [P_i]/(K_d \times K_p \times \text{Den}) - V_r^{max} \times [ATP]/(K_a \times \text{Den}) \quad (2)$$

where V_f^{max} and V_r^{max} are the maximum rates in the forward (ATP synthesis) and reverse (ATP hydrolysis) reactions, respectively. Den designates the denominator of the expression

$$\text{Den} = 1 + [ADP]/K_d + [ADP] \times [P_i]/(K_d \times K_p) + [ATP]/K_a \quad (2a)$$

[ADP], [P_i], and [ATP] designate the concentrations of these metabolites in the matrix space. The steady-state concentration of P_i in matrix space has been assumed to be 10-fold higher (Giesen and Kammermeier, 1980) than the levels in the mitochondrial intermembrane space at each time step.

Adenine nucleotide translocase

ATP export by adenine nucleotide translocase (ANT) was taken to be equal to ATP production by ATP synthase: for this case the maximum rate of ATP production by ATP synthase was assumed to be equal to the maximum rate of ANT activity. Thus, as a first approximation, it was assumed that ANT functions in a rapid equilibrium state, providing a constant ATP/ADP ratio between the matrix and intermembrane space at a fixed membrane potential (according to the concept of Wilson and Erecinska and several others, as reviewed by Hassinen, 1986). The ANT-provided steady-state concentration of ADP in matrix space has been assumed to be about 25-fold higher than the levels in the mitochondrial intermembrane space at each time step, because of the electrogenicity of the ADP-ATP exchange reaction (Klingenberg and Rottenberg, 1977). The sum of [ADP] and [ATP] in the matrix space, $[ANP]_m$, was taken to be a constant (10 mM). At each time step the steady-state ratio between ATP and ADP concentrations in the mitochondrial matrix (m) and intermembrane (im) spaces (Klingenberg and Rottenberg, 1977), $([ATP]_{im}/[ADP]_{im})/([ATP]_m/[ADP]_m)$, was assumed to be constant (25). So:

$$[ADP]_m = [ADP]_{im} \times [ANP]_m/([ADP]_{im} + [ATP]_{im}/25) \quad (2b)$$

$$[ATP]_m = [ANP]_m - [ADP]_m \quad (2c)$$

Simple diffusional coupling between mitochondrial creatine kinase and adenine nucleotide translocase

Functional coupling of mitochondrial creatine kinase and adenine nucleotide translocase is a well-documented phenomenon (Wallimann et al., 1992; Koretsky, 1995; Saks et al., 1975, 1985, 1995, 1996; Saks and Ventura-Clapier, 1994; Jacobus and Saks, 1982). For its mathematical modeling we have developed a probability approach describing in detail fluxes of adenine nucleotides both into and out of mitochondria (Aliev and Saks, 1993, 1994). It is a most detailed model of coupled reactions in mitochondria; however, its use in the frame of a complete model of cellular energy metabolism is not easy because of the very large number of necessary calculations. This is why we have simplified, at this step of modeling, the mathematical description of this central process of compartmentalized energy transfer: functional coupling in mitochondria. For this simplification we have used the experimental data of Fossel and Hoefeler (1987), which show that the phenomenon of functional coupling between enzymes appears if the distance between them is smaller than 10 nm. This was taken to be the maximum size of a gap (microcompartment) between the mitochondrial creatine kinase and adenine nucleotide translocase in which the local ATP concentration is increased because of metabolic channelling. In this gap the functional coupling was modeled by assuming a specific retardation of ATP diffusion in a 10-nm narrow space between coupled molecules (Fig. 1). ATP concentration in this gap was calculated in the following way.

In the space between translocase and creatine kinase, the ATP transported by ANT during the time interval dt increases the ATP concentration by ($\Delta[ATP]_{ANT}$). On the other hand, ATP partly diffuses out of the gap, decreasing the ATP concentration by ($\Delta[ATP]_{Dif}$). Moreover, part of the ATP is consumed by mitochondrial creatine kinase that decreases the ATP concentration by ($\Delta[ATP]_{CKm}$) (Fig. 1). The net change in local ATP concentration in the gap, ($\Delta[ATP]_{loc}$), is determined by the difference between ATP influx and efflux,

$$\Delta[ATP]_{loc} = \Delta[ATP]_{ANT} - \Delta[ATP]_{CKm} - \Delta[ATP]_{Dif} \quad (3)$$

Equation 3 was used for the calculation of the local ATP concentration ($[ATP]_{loc}$) in the gap. For this purpose the terms of Eq. 3 were calculated or expressed as a function of $[ATP]_{loc}$; their reintroduction into Eq. 3 easily gave a solvable quadratic equation with the only unknown, $[ATP]_{loc}$. This final expression is too long for presentation, so it seems reasonable to show the means of the opening of these terms.

$\Delta[ATP]_{loc}$, the change in the local ATP concentration in the gap, is the difference between local ATP concentrations at the time $t + \Delta t$, ($[ATP]_{loc}$), and the preceding time point t, ($[ATP]_{loc0}$) (0 meaning old concentration):

$$\Delta[ATP]_{loc} = [ATP]_{loc0} - [ATP]_{loc} \quad (4)$$

The flux of ATP from ANT has been assumed to be equal to the rate of net ATP synthesis by ATP synthase. So for Δt (the time interval) the change in local ATP concentration due to ATP influx from ANT, $\Delta[ATP]_{ANT}$, is

$$\Delta[ATP]_{ANT} = v_{net}^{syn} \times \Delta t \quad (5)$$

$\Delta[ATP]_{CKm}$, the ATP consumption by CK_{mit} during the time interval Δt, is

$$\Delta[ATP]_{CKm} = v_{net}^{CKmit} \times \Delta t \quad (6)$$

v_{net}^{CKmit} is calculated from $[ATP]_{loc}$ and ADP, Cr, and PCr concentrations in the intermembrane space according the kinetic equation for the creatine kinase reaction (Saks et al., 1975; Jacobus and Saks, 1982).

$\Delta[ATP]_{Dif}$, the diffusional efflux of ATP from the gap, can be estimated from the equations for restricted diffusion. Fig. 2 *B* shows the proposed profiles of ATP concentrations in the gap (ATP_{loc}), at its outer boundary (ATP_{out}), and in the intermembrane space (ATP_{i3}). ATP diffusion in the gap (space between ATP_{loc} and ATP_{out} points) is restricted by the given coefficient, resg (resistance for ATP diffusion in the gap space). The value of this coefficient will be estimated from the experimental data on changes in creatine kinase reaction characteristics induced by oxidative phosphorylation. The ATP concentration profile in this gap is assumed to be symmetrical (Fig. 2 *B*). Thus, according to Eqs. 1c and 1a, the diffusional changes in $[ATP]_{out}$ and $[ATP]_{loc}$ during the time interval Δt can be expressed as

$$\Delta[ATP]_{out} = r1 \times ([ATP]_{i3}^t - [ATP]_{out}^t) - r1 \times resg \times ([ATP]_{out}^t - [ATP]_{loc}^t) \quad (7)$$

$$\Delta[ATP]_{loc} = r1 \times resg \times ([ATP]_{out}^t - [ATP]_{loc}^t) \times 2 \quad (8)$$

In these equations $r1 = D_{ATP} \times \Delta t/\Delta l_1^2$; D_{ATP} is the diffusion coefficient for ATP; Δt is the time increment; Δl_1 is the distance between two adjacent space points in the diffusion path (Fig. 2 *B*).

At the steady state, $\Delta[ATP]_{out} = \Delta[ATP]_{loc}$. Equalizing the right sides of Eqs. 7 and 8 gives the expression for $[ATP]_{out}^t$:

$$[ATP]_{out}^t = (ATP_{i3}^t + 3 \times ATP_{loc}^t \times resg)/(1 + 3 \times resg) \quad (9)$$

Substituting $[ATP]_{out}^t$ in Eq. 8 by its expression in Eq. 9, we obtain Eq. 10:

$$\Delta[ATP]_{loc} = \Delta[ATP]_{Dif} = 2 \times r1 \times resg \times ([ATP]_{i3}^t - [ATP]_{loc}^t)/(1 + 3 \times resg) \quad (10)$$

Kinetics of ATP hydrolysis by myofibrils during contraction

The proposed kinetic scheme of ATP hydrolysis in myofibrils, a linear increase in the ATP hydrolysis rate up to 30 ms (t_1), followed by its linear

decrease to zero at 60 ms (t_2), has a simple analytical solution:

$$ATP_h = Acl \times t_1^2 \times 0.5 + Dcl \times (t_2 - t_1)^2 \times 0.5 \quad (11)$$

where ATP_h is the total amount of hydrolyzed ATP per cardiac cycle; Acl is the coefficient of the acceleration in ATP hydrolysis rate during the time period $0 - t_1$; Dcl is the coefficient of the deceleration in ATP hydrolysis rate during the time period $t_2 - t_1$.

The Acl and Dcl coefficients are interrelated:

$$Dcl = Acl \times t_1/(t_2 - t_1) \quad (12)$$

Taken together, Eqs. 11 and 12 can be used to calculate Acl (and hence Dcl):

$$Acl = ATP_h \times 2/(t_1 \times t_2) \quad (13)$$

Acl and Dcl, multiplied by time t in the time period $0 - t_2$, give the ATP hydrolysis rate for myofibrils. Hence the amount of hydrolyzed ATP during the time interval Δt (ΔATP_h) is

$$\Delta ATP_h = Acl \times t \times \Delta t \quad (14)$$

for the time period $0 - t_1$, and

$$\Delta ATP_h = Dcl \times (t_2 - t) \times \Delta t \quad (15)$$

for the time period $t_1 - t_2$.

Choice of the parameters for modeling

The accepted values of parameters are listed in Table 1. In this model we calculate directly the metabolite concentrations at each point in the diffusion path. Such a calculation of diffusion events in a plane sheet (Crank, 1975) supposes the proportionality between the unit of diffusion path length and the space volume, corresponding to this unit. In other words, if the diffusion path lengths in myofibrillar, cytoplasmic, and mitochondrial intermembrane spaces (MIS) are in the proportions 10:2:1, such proportionality should preexist in the volumes of these compartments. From the morphometric data of Page (Smith and Page, 1976), taking into account 81.5% of the cardiomycyte's volume in intact rat heart (Smith and Page, 1976; Anversa et al., 1979), the volumes of myofibrillar, cytoplasmic, and MIS compartments can be estimated as 380.6, 79.1, and 39.4 ml · (kg wet mass)$^{-1}$, respectively. The proportions between rounded fractional volumes (FV, L · (L tissue)$^{-1}$) of these compartments is 0.400:0.080:0.040 = 10:2:1. At a cardiac myofibril radius of 1.0 μm (Meyer et al., 1984), the unit of diffusion path length may be taken as 1.0 μm/10 parts = 0.1 μm. With this unit, diffusion path lengths in myofibrillar, cytoplasmic, and mitochondrial intermembrane compartments can be taken as 1.0, 0.2, and 0.1 μm, respectively, at a proportion 1.0 μm:0.2 μm:0.1 μm = 10:2:1 (Fig. 1). In the model the minimum diffusion path (0.1 μm) for mitochondrial outer membrane was artificially placed in the cytoplasmic compartment (Fig. 1) to maintain the total diffusion accessible space, which is 380.6 + 79.1 + 39.4 = 499.1 ml · (kg wet mass)$^{-1}$. With a total diffusion-accessible space of ~0.5 L · (kg wet mass)$^{-1}$, the known metabolite contents in tissue (mmol · (kg wet mass)$^{-1}$) should be multiplied by 2 to obtain the real concentration values (mM) in diffusion spaces (Table 1). These concentrations were taken from chemical and NMR data on metabolite contents and concentrations in rat heart muscle (see Saks et al., 1994).

In a compartmentalized system, each enzyme operates in its compartment, so that the maximum activities of enzymes should be normalized to the volumes of corresponding compartments. This was done by dividing the value of the maximum activity of enzymes in the tissue (mmol · s^{-1} · (kg wet mass)$^{-1}$) by the fractional volumes (FVs) of the compartments, listed in Table 1. Such normalization has also been performed for the value of ATP, hydrolyzed in myofibrils during contraction (Table 1).

The maximum activities of enzymes in in vivo rat heart at 37°C were taken from multiple biochemical data on enzyme distribution, their stoichiometries, and catalytic constants (see Saks et al., 1994). The accepted maximum rate of ATP export by mitochondrial ANT (Table 1) at $ATP/O_2 = 6$ corresponds (71.1 ml of O_2 · min^{-1} · (100 g tissue)$^{-1}$) to the upper limit of 54–72 ml of O_2 · min^{-1} · (100 g tissue)$^{-1}$) estimated by Elzinga and van der Laarse (1990). This is in good agreement with many other data (Saks et al., 1994; Williamson et al., 1976). With commonly used mitochondrial protein content in rat heart, 60 mg · (g wet mass)$^{-1}$, the predicted maximum rate of ATP production by in vivo mitochondria is 3.18 μmol ATP · min^{-1} · (mg protein)$^{-1}$. The experimental value for isolated mitochondria is somewhat lower, 2.1–2.4 μmol · min^{-1} · (mg protein)$^{-1}$ (Saks, 1980). The accepted value of maximum ATP production by CK_{mit} plus CK_{myo} (42.7 mmol · s^{-1} · (kg wet mass)$^{-1}$, see Table 1) coincides with the experimental value of Ventura-Clapier et al. (1987), 9.9 ± 0.5 μmol · min^{-1} · (mg fiber protein)$^{-1}$ at 30°C, if we correct the value by the temperature coefficient (1.75; Bittl et al., 1987), the actual substrate concentrations during measurement (Ventura-Clapier et al., 1987; Bittl et al., 1987), and the protein content in fiber (110 mg · (g wet mass)$^{-1}$). Bittl et al. (1987) estimated this parameter as 40.6 mmol · s^{-1} · (kg wet mass)$^{-1}$.

Based on the essential similarity in structure, and equal diffusibility of ADP and ATP molecules, the in vivo permeabilities of mitochondrial outer membrane for ATP and ADP have been assumed to be equal, $resm_{ATP} = resm_{ADP}$. For the case of restricted permeability of the outer mitochondrial membrane, the values of these constants were calculated to fit the experimentally determined apparent K_m for ADP in the regulation of mitochondrial respiration in permeabilized cardiomyocytes or skinned fibers, equal to 400 μM (Saks and Ventura-Clapier, 1994; Saks et al., 1995) (see Table 1).

Most important, however, is a reliable determination of the restricted diffusion coefficient for ATP from the gap, or microcompartment, between ANT and CK_{mit}. For this we used the experimental data obtained from isolated heart mitochondria when the creatine kinase reaction was studied under conditions of oxidative phosphorylation. It was shown by Saks et al. (1985), Soboll et al. (1992, 1994), and Jacobus and Saks (1982) that oxidative phosphorylation induces a shift in the creatine kinase mass action ratio from the equilibrium constant value and alters the kinetic constant, K_a, for the dissociation of ATP from the ternary complex E · Cr · ATP, decreasing it from 0.15 to 0.014 mM (Jacobus and Saks, 1982). These changes were explained well by a probability model (Aliev and Saks, 1993). In this work we assumed that these definite changes are due to elevated local ATP concentrations in the gap between ANT and MiCK, which increases because of the activity of ANT and decreased diffusion of ATP out of this gap, due to its specific structure, and intermediate binding to the active or binding centers. Thus we used the model described here, giving the different values of resg coefficient, and calculated the rates of mitochondrial creatine kinase reaction, comparing the calculated results with the curve obtained on the basis of experimental data. The best fit was found at a value of resg = 3×10^{-6}, and this value was used in all calculations.

Arrangement of calculations

In this model we calculate directly the time- and space-dependent changes in metabolite levels in in vivo working heart cells. Based on the known metabolite levels at a given time t, we determine the rates of concentration changes from diffusion and enzyme activities. These rates, multiplied by the value of a given Δt time change, give the absolute value of a concentration change during the Δt period. These values, when summed up with preexisting concentration values at each point of diffusion pathway, give the new space profile of concentrations at a new time point, $t + \Delta t$. The calculation cycles are repeated until attainment of a steady state, when the time profiles of any metabolite concentrations (see, for example, Fig. 5) coincide in each contraction cycle.

Throughout the program, the maximum enzyme activities were normalized by the FV value of relative volume of the compartment (Table 1). Besides the equations for diffusion, the Runge-Kutta algorithm was used in numerical calculations of the rates of enzymatic events. In these cases the steady-state equations for enzymatic velocities (equations 2 and 13 in Saks

TABLE 1 Parameters for modeling

Event	Parameter	Equation	Dimension	Value	Source
Diffusion	D_x	1, 1a–1d, 7–10	cm^2*s^{-1}	$D_{ATP} = D_{ADP} = 1.45 \times 10^{-6}$	Meyer et al. (1984)
				$D_{PCr} = D_{Cr} = 2.6 \times 10^{-6}$	Meyer et al. (1984)
				$D_{Pi} = 3.27 \times 10^{-6}$	Meyer et al. (1984)
	Δl	1, 1a–1d	cm	1×10^{-4}	
	Δl_1	7–10	cm	1×10^{-5}	
	Δt	1, 1a–1d, 7–10	s	1×10^{-5}	
	resm	1c, 1d		0.007 or 0.014	*
	resg	7–10		3×10^{-6}	
	C_j^t	1, 1a–1d	mM	$[ATP]_j^t = 9 - [ADP]_j^t$	
				$[ADP]_j^t = \Delta[ADP]_j$	#
				$[PCr]_j^t = 23 - [Cr]_j^t$	
				$[Cr]_j^t = 2 + \Delta[PCr]_j$	#
				$[P_i]_j^t = [ADP]_j^t + ([Cr]_j^t - 2)$	
ATP hydrolysis in myofibrils	ATP_h	11–13, 15	$mmol*(kg\ wm)^{-1}$	0.414	Wikman-Coffelt et al. (1983)
	t_1	11–13, 15	s	3×10^{-2}	
	t_2	11–13, 15	s	6×10^{-2}	
	FV		$L*(L\ tissue)^{-1}$	0.4	
CK_{myo}	V_1 (ADP production)	§§	$mmol*s^{-1}*(kg\ wm)^{-1}$	6.886	
	V_{-1} (ATP production)	§§	$mmol*s^{-1}*(kg\ wm)^{-1}$	29.333	
	K_x	§§	mM	K_{ia} (ATP) = 0.9	Saks et al. (1984)
				K_{ib} (Cr) = 34.9	§
				K_b (Cr) = 15.5	Saks et al. (1976)
				K_{id} (PCr) = 4.73	¶
				K_d (PCr) = 1.67	Saks et al. (1976)
				K_{ic} (ADP) = 0.2224	‖
				$K_{Ib} = K_{ib}$	Kupriyanov et al. (1984)
	FV			0.44	
CK_{mit}	V_1 (ADP production)	§§	$mmol*s^{-1}*(kg\ wm)^{-1}$	3.175	
	V_{-1} (ATP production)	§§	$mmol*s^{-1}*(kg\ wm)^{-1}$	13.333	
	K_x	§§	mM	K_{ia} (ATP) = 0.75	Jacobus and Saks (1982)
				K_{ib} (Cr) = 28.8	Jacobus and Saks (1982)
				K_b (Cr) = 5.2	Jacobus and Saks (1982)
				K_{id} (PCr) = 1.6	Jacobus and Saks (1982)
				K_d (PCr) = 0.5	Saks et al. (1976)
				K_{ic} (ADP) = 0.2048	‖
				$K_{Ib} = K_{ib}$	Kupriyanov et al. (1984)
	FV		$L*(L\ of\ tissue)^{-1}$	0.004	**
ATP synthase	V_1 (ATP production)	2	$mmol*s^{-1}*(kg\ wm)^{-1}$	3.175	
	V_{-1} (ATP hydrolysis)	2	$mmol*s^{-1}*(kg\ wm)^{-1}$	0.028	
	K_x	2, 2a	mM	K_a (ATP) = 0.462	##
				K_d (ADP) = 0.1	##
				K_p (P_i) = 2.4	##
	FV		$L*(L\ of\ tissue)^{-1}$	0.004	**
	C_x^t	2, 2a	mM	$[ADP]^t$ from Eq. 2b	
				$[P_i]^t = [P_i]_{13}^t \times 10$	
				$[ATP]^t = 10 - [ADP]^t$	

*resm values of 0.007 and 0.014 provide an apparent K_m for ADP of 400 and 200 μM, respectively, at state 3 respiration.

#$\Delta[ATP]_j$ and $\Delta[PCr]_j$ represent integral ATP and PCr expenditures, respectively, before time t at space point j.

§K_{ib} was calculated from the thermodynamic equation $K_{ib} \times K_a = K_{ia} \times K_b$ at $K_a = 0.4$ mM (Saks et al., 1984).

¶K_{id} was calculated from the thermodynamic equation $K_{id} \times K_c = K_{ic} \times K_d$ with $K_{ic}/K_c = 2.833$ (Saks et al., 1984).

‖K_{ic} value has been settled to obtain the apparent equilibrium constant of CK reaction 6.25×10^{-3}.

**This coefficient takes into account the location of CK_{mit} and ANT in an extremely narrow space between these molecular complexes.

##Values were taken from our analysis of the data of Holian et al. (1977) and Gyulai et al. (1985).

§§Activities of creatine kinases were calculated from equation 13 of Saks et al. (1975). The forward flux of creatine kinase (v_f) was calculated by the equation $v_f = V_1*[ATP]*[Cr]/(K_{ia}*K_b*Den)$, and the reverse flux of creatine kinase (v_r) from $v_r = V_{-1}*[ADP]*[PCr]/(K_{ic}*K_d*Den)$. The net flux through creatine kinase (v_{net}) was $v_{net} = v_f - v_r$. In these equations Den designates **Den**ominator, which is $Den = 1 + [ATP]/K_{ia} + [ADP]/K_{ic} + [Cr]/K_{ib} + [PCr]/K_{id} + [ATP]*[Cr]/(K_{ia}*K_b) + [ADP]*[PCr]/(K_{ic}*K_d) + [ADP]*[Cr]/(K_{ic}*K_{Ib})$. The values of the constants are listed in this table.

et al., 1975) were used as differential ones. The Runge-Kutta algorithm provides high accuracy and stability in numerical calculations.

In the model the equations for steady-state activity were used in the calculations of the immediate changes of enzyme activities during extremely small time intervals Δt. This simplified approach is justified for enzymes with a rapid equilibrium binding mechanism and rate limitation at catalytic steps, such as creatine kinase (Cleland, 1967; Kenyon and Reed, 1983).

The attained data were used for the estimation of diffusion fluxes through the mitochondrial outer membrane. The fluxes (F_x) of x species of metabolites were calculated from their concentrations, C_x^{11} and C_x^{12}, on both sides of the mitochondrial outer membrane:

$$Fx = (C_x^{11} - C_x^{12}) \times \mathrm{resm}_x \times D_x/\Delta l^2 \times FV \qquad (16)$$

FV = 0.04 is an assumed fractional volume of mitochondrial outer membrane.

All calculations were carried out on a 486DX2-50 computer, in which the calculation of one contraction cycle takes 200 s. The program, written for Turbo Pascal, Version 7.0, is too large to be shown in this paper, but is available from M. K. Aliev on request.

RESULTS

Testing the model: fitting with experimental data

For testing of the correctness of the model, we used the published experimental results by Holian et al. (1977) and Gyulai et al. (1985). In the work of Holian et al. (1977), isolated pigeon and dog heart mitochondria were tested in vitro for the quantitative dependence of the respiratory rate on the extramitochondrial ATP, ADP, and P_i concentrations. The dependence of respiration rate on the ADP concentration at different fixed ATP and constant P_i concentrations, taken from the work by Holian et al. (1977), is shown in Fig. 3 *A*, in double-reciprocal plots using separate symbols: the solid lines show the results of simulating this dependence, by using our model described in Methods. Clearly, the results of the simulation fit the experimental results well. In all cases, there is practically no deviation of calculated lines from experimental points. This means that the part of the model describing the mitochondrial ATP synthase-ANT- phosphate carrier complex and their interaction with cytoplasmic (extramitochondrial) substrates is correct.

Most interesting, however, is the classical work from the Chance laboratory, published by Gyulai et al. (1985). In this work, the authors tried to "bridge the gap between in vitro experiments, in which added or generated ADP regulated mitochondrial activity, and in vivo experiments, in which phosphocreatine and creatine kinase are present and respiration is set by the ATPase activity accompanying cellular work at different rates." They therefore studied isolated rat heart mitochondria containing CK_{mit} in a medium containing substrates, PCr, Cr, ATP, P_i, and Mg^{2+} at the concentrations expected for in vivo conditions. The ATPase activity was varied by the addition of potato apyrase, and changes in extramitochondrial phosphorus compounds were followed by ^{31}P-NMR. This elegant work is perfect for our purpose of testing the main part of the model, including mitochondria and the activated creatine kinase system, with ATPase as the source of ADP. The authors calculated the logarithm of the phosphorylation ratio (or potential, as it is sometimes called), log ([ATP]/([ADP] · [Pi])) as a function of the ATPase rate. We did the same by using our model, normalizing the activity with respect to the maximum rates, V_{max}. The results by Gyulai et al. (1985) are shown by open diamonds in the upper part of Fig. 3 *B*, and the solid line shows the simulated dependence. The fitting between experimental and simulated dependences seems to be perfect.

The lower curve in Fig. 3 *B* shows similar results (*symbols*) taken from the work by Holian et al. (1977), where in both experiments and calculations, CK_{mit} was not activated (no Mg^{2+} was present) and there was no ATPase activity. In this case there is also a good fit between experimental and simulated results. The remarkable difference between these two groups of data is due to activation of CK_{mit} in the case of the work by Gyulai et al. (1985)—in this case a high local ATP concentration generated by ANT maintains high steady-state concentrations of PCr in the medium, reflecting a very high local ATP/ADP ratio in the vicinity of the CK_{mit} active site (Saks et al., 1985; Soboll et al., 1992, 1994).

Thus the model developed in this work adequately describes the available in vitro data. Therefore it is reasonable to use this model for analyzing the energy metabolism of the cell under in vivo conditions.

Changes of energy profiles and metabolic fluxes within contraction cycle: effects of restricted diffusion of adenine nucleotides through the outer mitochondrial membrane

Fig. 4 shows the calculated changes in the profiles of energy metabolites in the core of myofibrils during the cardiac cycle. In this system there is a restricted diffusion of adenine nucleotides through the mitochondrial outer membrane for normal cardiomyocytes at relatively high workloads. The calculated changes are shown as deviations from the resting level and are given in μM. Resting and peak values of metabolite concentrations are listed in Table 2. The calculations show that activation of contraction results in a small transient decrease in ATP and a symmetrical increase in ADP, followed by deeper and longer changes in PCr and Cr concentrations. Changes in the levels of adenine nucleotides are rapid and occur within 90 ms. P_i concentration changes in a way similar to that of free Cr. By the end of the contraction cycle, however, all metabolite levels are restored to their initial value. Because of high initial values for the ATP, Cr, and PCr concentrations, their relative changes in the contraction cycle are within the range of several percent (about 4% for PCr; Table 2).

In the system without restricted diffusion of adenine nucleotides through the mitochondrial outer membrane, the changes are similar, except for smaller and faster changes in ADP concentrations, which reach the maximum peak value of 205 μM (Fig. 5, Table 2). Restriction of movement of adenine nucleotides across the mitochondrial membrane

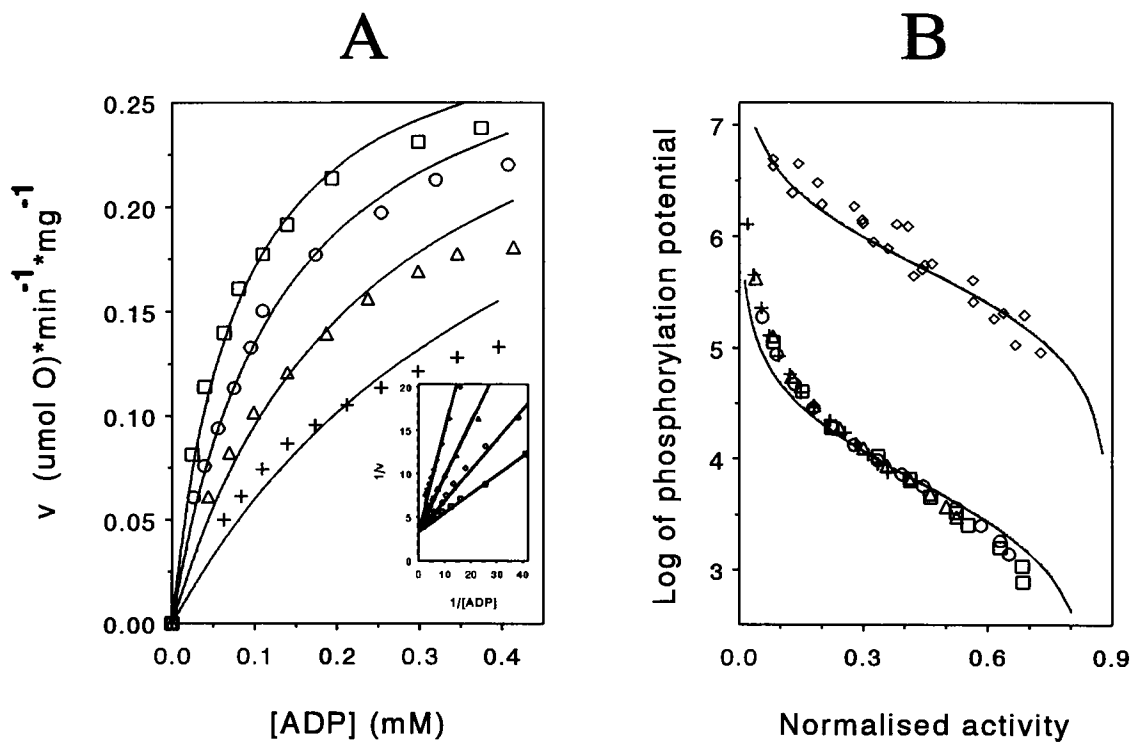

FIGURE 3 Experimental (*symbols*) and simulation (*lines*) data on kinetic and thermodynamic behavior of reconstituted in vitro systems of mitochondrial oxidative phosphorylation. (*A*) Double-reciprocal plots of [ADP] dependence of oxygen consumption rates by heart mitochondria at constant initial [P_i], 4 mM, and varying fixed initial [ATP]: 1 mM (□), 2 mM (○), 4 mM (△), and 8 mM (+). Experimental data (*symbols*) were taken from figure 2 *B* of Holian et al. (1977). In that work, phosphorylation was initiated at a room temperature upon the addition of 600 μM ADP to the oxygenated incubation mixture with 200 mM sucrose, 5 mM glutamate, 5 mM malate, indicated concentrations of P_i and ATP, 1.12 mg · ml^{-1} of pigeon heart mitochondria protein, and 25 mM 3-(*N*-morpholino)propanesulfonic acid at pH 7.0 (Holian et al., 1977). Oxygen consumption rates were recorded continuously upon phosphorylation of added ADP. From these data we calculated the ADP levels at different oxygen consumption rates from the relative residual area of the time-velocity integral, the total area of which was assumed to correspond to 600 μM [ADP]. The calculated ADP, ATP, and P_i concentrations correspond to those obtained by direct chemical determinations. Simulated data (*lines*) were obtained at parameters indicated in Table 1 for ATP synthase, except that K_d(ADP) = 4.2 mM, $K_p(P_i)$ = 4.8 mM, V_1 = 0.34 μmol O · min^{-1}, $V_{-1} = V_1/9584.8$. (*B*) Steady-state values of extramitochondrial log phosphorylation ratio asa function of respiration (*lower part*; Holian et al., 1977) or total ATPase (*upper part*; Gyulai et al., 1985) activities. Phosphorylation potential is defined as log ([ATP]/([ADP] · [P_i])). Experimental (*symbols*) and simulated (*lines*) data for the lower part of the figure are those for Fig. 3 *A* (data of Holian et al., 1977); the activities were normalized by V_1 = 0.34 μmol O · min^{-1}. Experimental data for the upper part of the figure (◇) were taken from figure 3 of Gyulai et al. (1985). Phosphorylation was initiated at 25°C upon the addition of 0.5–2 mg · ml^{-1} of rat heart mitochondria protein to the oxygenated incubation mixture with 125 mM sucrose, 40 mM KCl, 5 mM pyruvate, 5 mM malate, 10 mM Na_2ATP, 13 mM $MgCl_2$, 18 mM PCr, 5 mM HEPES, 20% D_2O in H_2O at pH 7.2 (Gyulai et al., 1985). The mixture was supplied with different amounts of potato apyrase to attain desired rates of extramitochondrial ATP hydrolysis. On attaining steady-state ATP hydrolysis, the phosphorus compounds were determined by ^{31}P-NMR. The steady-state ATPase rates (which are equal to steady-state rates of oxidative phosphorylation) were normalized by V_{max} = 0.82 μmol · min^{-1} · mg^{-1} (Gyulai et al., 1985). Simulated data (*lines*) for the upper part of the figure were obtained at parameters indicated in Table 1 for ATP synthase.

results in a higher ADP peak value of 383 μM, and in both cases the resting ADP value is very low.

Metabolic fluxes in different cellular compartments

Alterations of the concentrations of metabolites within one contraction cycle (shown in Fig. 4) are due to different enzymatic reactions in various cellular compartments and metabolic fluxes between these compartments. These calculated compartmentalized fluxes are shown in Fig. 6 as the rates of net ATP synthesis in mitochondrial matrix by ATP synthase, in the coupled mitochondrial creatine kinase reaction and by the myofibrillar creatine kinase reaction. It is the latter reaction that is most significantly activated within the contraction cycle and which restores myofibrillar levels of adenine nucleotides within 60–90 ms (see Figs. 4 and 5) at the expense of PCr. Zero net synthesis of ATP in the creatine kinase reaction corresponds to the equilibrium position of this reaction, and Fig. 6 shows that it is practically never completely achieved—only in the diastolic phase of the contraction cycle is the myofibrillar creatine kinase reaction in a quasiequilibrium state, at a minimum constant rate of ATP utilization (Fig. 6). In the mitochondrial creatine kinase reaction, net ATP synthesis is negative—this reaction continuously uses mitochondrial ATP to produce PCr by a mechanism of functional coupling between creatine kinase and translocase in heart mitochondria (Wallimann et al., 1992; Saks et al., 1975, 1996). Therefore, this reaction is never in the equilibrium state, and its steady-state

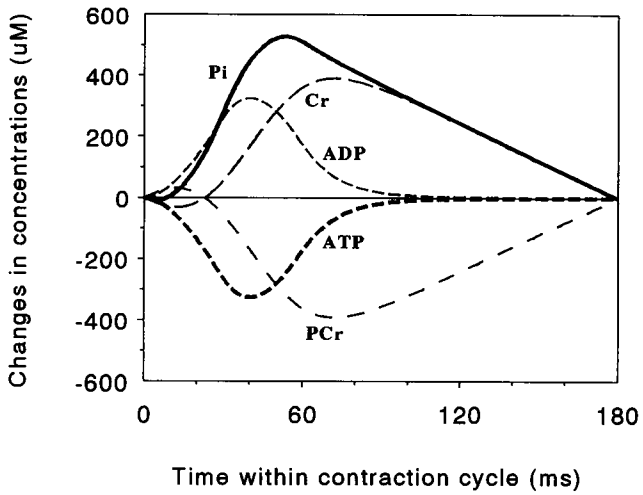

FIGURE 4 Phasic changes in metabolite concentrations in myofibril core during the cardiac contraction cycle: a system with restrictions for ATP and ADP diffusion through the mitochondrial outer membrane. The decrease in outer membrane permeability corresponds to an apparent K_m for ADP of 400 μM ($res_{ATP} = res_{ADP} = 0.007$).

rate depends on the permeability of mitochondrial outer membrane for adenine nucleotides. Because of the liberation of ADP in cytoplasm within the first part of the contraction cycle (see Figs. 4 and 5), this reaction may be shifted somewhat but not completely, in the direction of ATP synthesis, if the diffusion of adenine nucleotides across the outer mitochondrial membrane is not restricted. However, when mitochondrial outer membrane permeability for adenine nucleotides is restricted, this reaction becomes almost insensitive to ADP changes in myofibrillar space and produces PCr with a constant rate that is practically equal to the rate of ATP synthase reaction in the mitochondrial matrix and the steady-state rate of adenine nucleotide translocation. Obviously these coupled reactions of aerobic phosphocreatine production are responsible for the restoration of the PCr level by the end of the contraction cycle (Fig. 4). Restriction of adenine nucleotide diffusion across the outer mitochondrial membrane does not influence the maximum rate of net synthesis of ATP by ATP synthase, because the coupled mitochondrial creatine kinase reaction in the intermembrane space is a major source of ADP and hence a major factor in the control of respiration (Saks and Ventura-Clapier, 1994; Saks et al., 1995, 1996). However, restriction of ADP diffusion through the outer mitochondrial membrane does delay the activation of this reaction in the contraction cycle.

Fig. 7 shows one of the main results of our calculations on the basis of a model developed in this work: the energy fluxes from mitochondria carried by ATP and PCr. Comparison of Fig. 7, *A* and *B*, shows that restriction of the permeability of the outer mitochondrial membrane for adenine nucleotides significantly decreases the diffusional ATP export, as might be expected. This export may be rather significant in the first part of the contraction cycle if the diffusion is not restricted, but in the diastolic phase most of the energy is carried out of the mitochondria by PCr (Fig. 7 *A*). In the case of restricted diffusion, however, the ATP export becomes negligible (Fig. 7 *B*), and energy is carried out of the mitochondria almost exclusively by PCr. In this case it is the free Cr that metabolically connects the myofibrillar space to mitochondria.

Effects of "switch-off" of creatine kinase isoenzymes

Recently several important works have been published that describe the results of the creatine kinase gene manipulation producing transgenic mice with "knocked out" myoplasmic creatine kinase or CK_{mit} (van Deursen et al., 1993, 1994a,b). In particular, a detailed analysis was given by Veksler et al. (1995) of mitochondrial function in the skinned cardiac and skeletal muscle fibers after complete block of the synthesis of MM subunits of creatine kinase. The latter case is analyzed first in this section by using our generalized mathematical model. The activity of CK_{myo} in the myofibrillar space was taken to be zero, and the energy fluxes in mitochondria were calculated for the whole contractile cycle. Results of these calculations are described in Figs. 8 and 9 and in Table 2. These results show that the rate of ATP synthase is not changed, and ATP is synthesized at an unaltered rate after "knock-out" of creatine kinase (see Figs. 6 and 8). However, the mitochondrial creatine kinase reaction is changed in comparison to the normal case shown in Fig. 6. In the absence of CK_{myo} in the cytoplasmic space, mitochondrial creatine kinase responds to the contraction by changing the direction of the reaction in the beginning of the contraction cycle. This reaction switches from PCr production to ATP production (net ATP synthesis becomes positive), and the amplitude of this positive response is dependent on the diffusion of adenine nucleotides across the outer mitochondrial membrane: restriction of this diffusion decreases the amplitude of the response of mitochondrial creatine kinase (*solid lines*) to contraction and postpones its reversal to PCr production during the diastolic phase. Thus, in this case, within the first part of contraction cycle, mitochondrial creatine kinase, by producing ATP, functionally replaces myoplasmic creatine kinase and fulfills the double function of production and utilization of PCr.

Fig. 9 shows what may happen in the myofibrillar core in the case of inhibition of MM creatine kinase. As may be expected, such inhibition results in manifold elevation of the peak value of ADP in the core of myofibrils, which may reach 500 μM in the case of unlimited diffusion of ADP through the outer membrane of mitochondria. If the permeability of this membrane for adenine nucleotides is restricted, the free ADP concentration in the core of myofibrils may rise to 800 μM. This probably does not happen, because Veksler et al. have shown increased permeability of the outer mitochondrial membrane for ADP as an adaptive response to the "knock-out" of myoplasmic creatine kinase

TABLE 2 Resting levels (rest) and peak values (peak) of substrate concentrations achieved during the cardiac cycle in different simulated systems

System		Concentrations in myofibril core (mM)				
		P_i	ADP	ATP	PCr	Cr
Systems without diffusion restrictions on mitochondrial outer membrane						
Complete	Rest	4.8147	0.0162	8.9838	16.1995	6.8005
	Peak	5.3264	0.2045	8.7955	15.7533	7.2467
Without CK_{myo}	Rest	2.6706	0.0058	8.9942	18.3346	4.6654
	Peak	3.2024	0.4874	8.5126	18.1778	4.8222
Without CK_{mit}	Rest	10.8391	0.0258	8.9742	10.1824	12.8176
	Peak	11.3378	0.3073	8.6927	9.8256	13.1744
Without CK	Rest	1.0359	0.0394	8.9606	—	—
	Peak	1.5982	0.6065	8.3940	—	—
Systems with diffusion restrictions on mitochondrial outer membrane						
Complete	Rest	10.2273	0.0584	8.9416	10.8221	12.1779
	Peak	10.7543	0.3831	8.6169	10.4319	12.5681
Without CK_{myo}	Rest	1.6358	0.1540	8.8460	19.4973	3.5027
	Peak	2.1909	0.7743	8.2257	19.4245	3.5755
Without CK_{mit}	Rest	18.1472	0.2116	8.7884	3.0323	19.9677
	Peak	18.6749	0.7111	8.2889	2.8669	20.1331
Without CK	Rest	1.2093	0.2430	8.7570	—	—
	Peak	1.7752	0.8428	8.1572	—	—

Calculations were made for an oxygen consumption rate of 23 μmol/min/g of wet tissue, which corresponds to the maximum workload of the cardiac muscle (Saks et al., 1996; Elzinga and van der Laarse, 1990; Williamson et al., 1978).

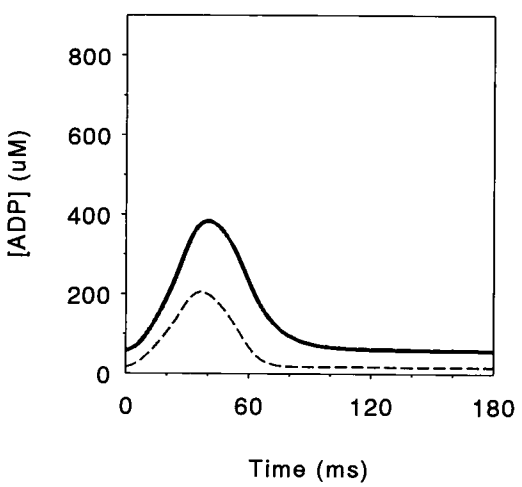

FIGURE 5 Dynamics of ADP concentration in myofibrillar core in the systems with (*solid lines*) or without (*dotted lines*) restrictions for adenine nucleotide diffusion through the mitochondrial outer membrane. The diffusion restrictions are as in Fig. 4.

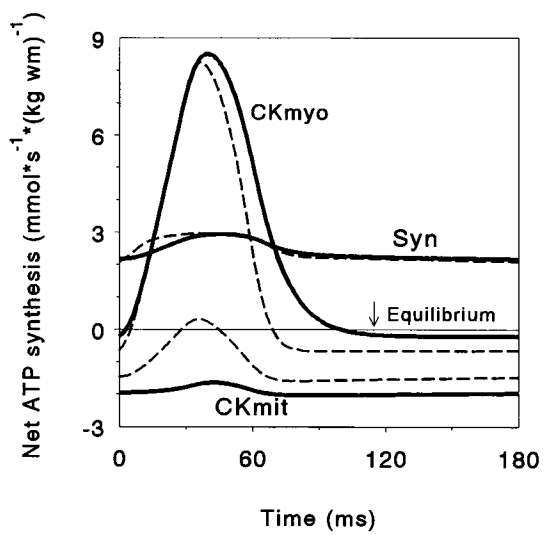

FIGURE 6 Nonequilibrium behavior of ATP synthase (Syn) and myofibrillar and mitochondrial CK (CK_{myo} and CK_{mit}, respectively) in the systems with (*solid lines*) or without (*dotted lines*) restrictions for adenine nucleotide diffusion through the mitochondrial outer membrane. An arrow indicates the position of equilibrium, when the net ATP production is equal to zero. The diffusion restrictions are as in Fig. 4.

(Veksler et al., 1995). The possible limit of the elevated ADP concentration in the core of myofibrils is around 500 μM in the case of nonrestricted diffusion of adenine nucleotides across the outer mitochondrial membrane (if other ADP-utilizing systems are not activated).

Another interesting case is the "knock-out" of the mitochondrial creatine kinase in transgenic animals (Steeghs et al., 1995). Mathematical modeling of this situation, when myoplasmic creatine kinase activity was taken to be normal and the activity of mitochondrial creatine kinase to be zero,

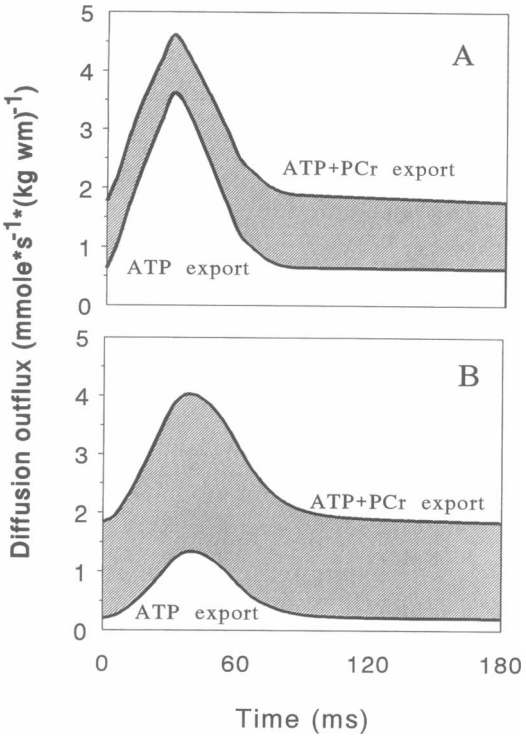

FIGURE 7 Diffusional ATP and PCr export through the mitochondrial outer membrane in the systems without (*A*) or with (*B*) restrictions for adenine nucleotide diffusion through the mitochondrial outer membrane. The shaded area indicates the PCr outflux. The diffusion restrictions are as in Fig. 4.

gave the results shown in Figs. 10 and 11, and in Table 2. First, the absence of mitochondrial creatine kinase significantly reduces the steady-state levels of the PCr in the cells

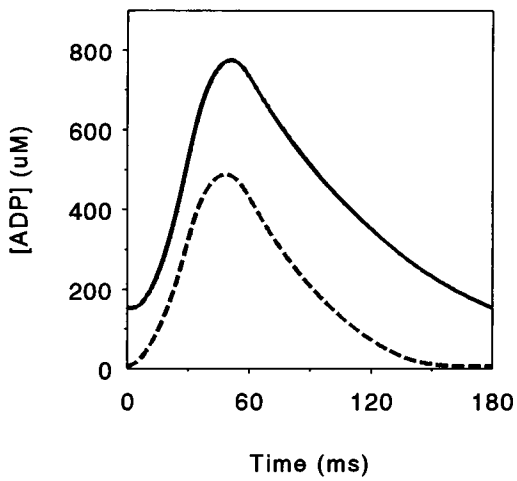

FIGURE 9 Dynamics of ADP concentration in myofibrillar core at the complete block of myoplasmic CK in the systems with (*solid line*) or without (*dotted line*) restrictions for adenine nucleotide diffusion through the mitochondrial outer membrane. Diffusion restrictions are as in Fig. 8.

(Table 2). Second, Fig. 10 shows that it is now the myoplasmic creatine kinase reaction that functions in two directions. Because of permanent steady-state production of ATP in mitochondria and the removal of ADP from cytoplasm, in the diastolic phase of the cardiac cycle the myoplasmic creatine kinase reaction produces PCr (negative rate of ATP synthesis). The price that the cell pays, however, for the absence of coupled reactions in mitochondria is at least a twofold decrease in the steady-state level of PCr in the cells. Within the contraction cycle, when actomyosin ATPase is activated and produces ADP, phosphocreatine is rapidly used in myofibrils for ATP production, and the direction of the reaction is reversed. In both cases, however, the creatine

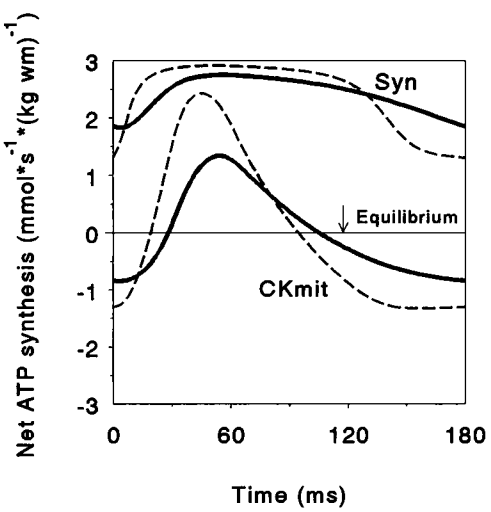

FIGURE 8 Behavior of ATP synthase (Syn) and mitochondrial CK (CK_{mit}) at the complete block of myoplasmic CK in the systems with (*solid lines*) or without (*dotted lines*) restrictions for adenine nucleotide diffusion through the mitochondrial outer membrane. The arrow indicates the position of equilibrium. The decrease in outer membrane permeability corresponds to an apparent K_m for ADP of 200 μM ($res_{ATP} = res_{ADP} = 0.014$).

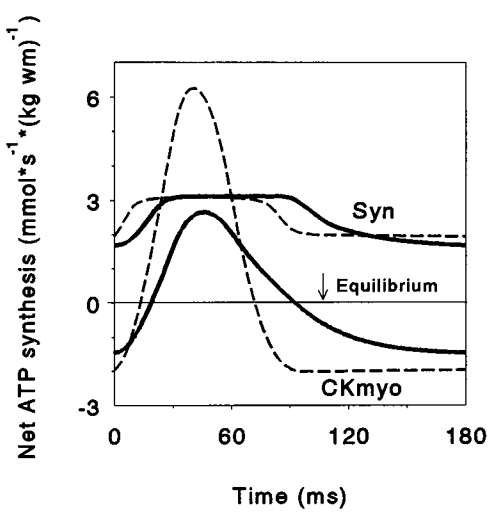

FIGURE 10 Behavior of ATP synthase (Syn) and myoplasmic CK (CK_{myo}) at the complete block of mitochondrial CK in the systems with (*solid lines*) or without (*dotted lines*) restrictions for adenine nucleotide diffusion through the mitochondrial outer membrane. The arrow indicates the position of equilibrium. Diffusion restrictions are as in Fig. 8.

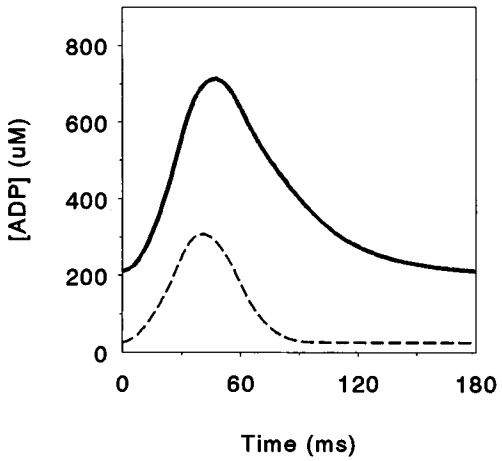

FIGURE 11 Dynamics of ADP concentration in the myofibrillar core at the complete block of mitochondrial CK in the systems with (*solid line*) or without (*dotted line*) restrictions for adenine nucleotide diffusion through the mitochondrial outer membrane. Diffusion restrictions are as in Fig. 8.

kinase reaction is far removed from the equilibrium position. Paradoxically, the rate of the myofibrillar creatine kinase reaction in the myoplasmic space now also depends on the permeability of the mitochondrial outer membrane for adenine nucleotides: restriction of adenine nucleotide diffusion through this membrane decreases the rate of myofibrillar creatine kinase reaction. This apparent paradox is explained by data given in Table 2. Restriction of the movement of adenine nucleotides through mitochondrial outer membrane decreases the rate of exchange of adenine nucleotides between mitochondria and cytoplasm, thus delaying the response of ATP synthase to contraction, decreasing the steady-state rate of PCr production and sharply decreasing the level of PCr to ~3 mM (Table 2). Correspondingly, the P_i level is significantly increased (Table 2). In the myofibrillar creatine kinase reaction, the value of K_m for PCr is 1.6 mM (Saks et al., 1976). In the complete system, because of competitive inhibition of PCr binding by ATP (because of the phosphate group overlap) and Cr (Cleland, 1967; Kenyon and Reed, 1983), the apparent K_m for PCr is elevated, and at 3 mM PCr the rate of its utilization is decreased. Thus this paradoxical effect has a kinetic explanation. Direct calculation of the ADP concentration in the cytoplasm (Fig. 11) shows that because of decreased exchange of adenine nucleotides between mitochondria and myoplasm, and the decreased rate of myoplasmic creatine kinase reaction, the calculated ADP level can reach a value of 711 μM in the case of restricted permeability of the outer mitochondrial membrane. In the case of nonlimited diffusion of adenine nucleotides, the maximum ADP concentration in the contraction cycle is 307 μM (Fig. 11, Table 2). Thus, in the case of the absence of the mitochondrial creatine kinase reaction, restricted permeability of the outer mitochondrial membrane for adenine nucleotides becomes a very negative factor in the life of the cell. This is also true for the case in which only myoplasmic creatine kinase is inhibited (Fig. 8). In these systems, a logical adaptive response of the cell is to increase the outer mitochondrial membrane permeability for ADP and ATP (see Veksler et al., 1995), and we may expect a very significant activation of the adenylate kinase system (Zeleznikar et al., 1995).

Finally, if the whole creatine kinase system is totally blocked, net mitochondrial ATP synthesis shows very significant variation during the contraction cycle (see Fig. 12, as compared to Figs. 6, 8, and 10). Even in the case of unlimited diffusion of ADP, its level rises very sharply, up to 606 μM, in the contraction cycle, and restriction of adenine nucleotide movement elevates ADP level further, up to 843 μM (Table 2, Fig. 13). Obviously this case is very dangerous for cell life if other adaptive processes that decrease the ADP level are not activated (see the Discussion).

From this analysis we can see that even in the case of restricted ADP diffusion, the complete creatine kinase system is able to keep cytoplasmic ADP concentrations reasonably low, also achieving stability of compartmentalized metabolic fluxes in mitochondria (see Fig. 6) and high efficiency of respiration regulation (Saks et al., 1996).

Changes in calculated energy fluxes and metabolic parameters with alteration of workload

Because the time resolution of available experimental techniques is not sufficient to precisely detect the changes in metabolic parameters throughout the cardiac cycle, we decided to model time-averaged parameters of energy metabolism as functions of energy demand (the workload). This creates the possibility of comparing the predictions of the model with published experimental data.

Fig. 14 shows the results of modeling of these time-averaged parameters. The steady-state rates of ATP utiliza-

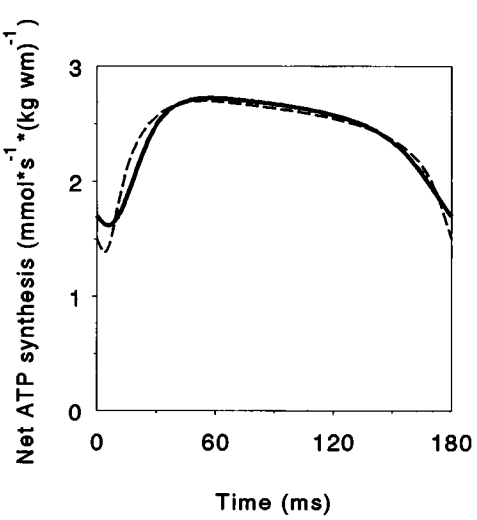

FIGURE 12 Behavior of ATP synthase at the complete block of myofibrillar and mitochondrial CK in the systems with (*solid line*) or without (*dotted line*) restrictions for adenine nucleotide diffusion through the mitochondrial outer membrane. Diffusion restrictions are as in Fig. 8.

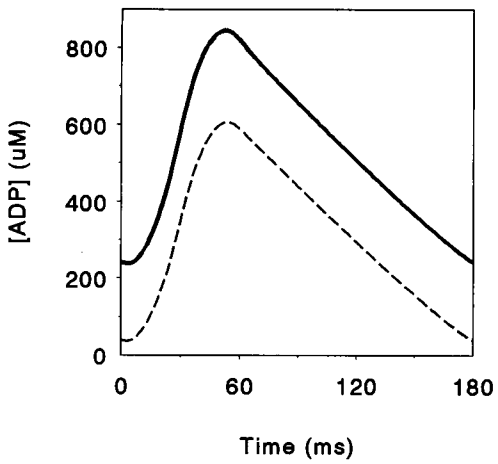

FIGURE 13 Dynamics of ADP concentration in the myofibrillar core at the complete block of myofibrillar and mitochondrial CK in the systems with (*solid line*) or without (*dotted line*) restrictions for adenine nucleotide diffusion through the mitochondrial outer membrane. Diffusion restrictions are as in Fig. 8.

tion and resynthesis were taken to change from 0 to 2.5 mmol $\times$ s^{-1} $\times$ (kg wet mass)$^{-1}$. The latter value corresponds to the maximum rate of oxygen consumption published in the literature (Wikman-Coffelt et al., 1983; Williamson et al., 1976). Fig. 14 *A* shows that our model predicts, for this range of workload, more than fourfold augmentation of the creatine kinase flux up to the rate of 4.3 mmol $\times$ s^{-1} $\times$ (kg wet mass)$^{-1}$, or about 24 μmol/g dry mass/s. This is in good agreement with the data of Perry et al. (1988), who used magnetization transfer NMR spectroscopy for estimation of the creatine kinase flux in isolated perfused adult rabbit heart at different levels of cardiac performance. In their work, a fourfold increase in the rate of ATP synthesis resulted in about a threefold acceleration of the creatine kinase flux (figure 2 in Perry et al., 1988). This is very close to our calculations (Fig. 14 A, *thick line*). For total creatine kinase, the calculated integral (time-averaged) forward and reverse fluxes are equal (Saks and Aliev, 1996). However, one can see from Fig. 14 *A* that for the myofibrillar creatine kinase reaction the difference between the reverse (ATP synthesis) and forward (phosphocreatine synthesis) steady-state fluxes increases with the elevation of the workload and is equal to the steady-state rate of ATP synthesis and utilization. Only at zero workload is this difference zero (Fig. 14 *A*). This means that the myofibrillar as well as mitochondrial creatine kinase reactions progressively deviate from the equilibrium with the elevation of the workload.

In Fig. 14 *A*, the thick line shows the values of creatine kinase fluxes in complete system, and in steady state the reverse and forward fluxes are equal. Thus the difference between total flux (*thick line*) and that of forward myoplasmic creatine kinase gives directly the forward mitochondrial creatine kinase flux, the rate of aerobic phosphocreatine synthesis in mitochondria. This flux increases with elevation of the workload, and its value is equal to that of the ATP synthesis (Fig. 14 *A*). Again, this result is in very good agreement (in fact, it completely fits the numbers) with the results of Ingwall's laboratory (Zahler et al., 1987; see figure 2 in Zahler and Ingwall, 1992).

Fig. 14 *B* shows the predictions of the model for the workload dependence of the PCr/ATP ratio, the parameter most frequently determined in phosphorus NMR studies of the heart. For the whole range of workload, the calculated PCr/ATP ratio changes from 2.4 to 1.2. This change is in good accord with the early results from Williamson's laboratory (Williamson et al., 1976). However, very numerous studies (reviewed by Saks et al., 1994) are in conflict with these results, and sometimes even an increase in the PCr/ATP ratio with elevation of the workload is observed (Wan et al., 1993). Thus our model describes well one group of experimental data, and further analyses of both the model and experimental data are obviously required to clarify this controversy.

Fig. 14 *C* shows the calculated time-averaged values (integrated for whole contraction cycle) of ADP concentration. Again, one can see that the difference between integrated and diastolic values of cytoplasmic ADP concentration increases with the increase in workload due to the deviation of the creatine kinase reaction from equilibrium. The intracellular concentration of phosphate increases with elevation of the workload (Fig. 14 *D*), because of the decrease in the phosphocreatine concentration (Fig. 14 *B*). The maximum calculated phosphate concentration may be in excess of experimental values of this parameter observed that show the necessity to develop further the part of the model that describes the feedback between contraction and respiration (see the Discussion).

In general, the calculated time-averaged values of the metabolic parameters approach the results of multiple experimental investigations. And this means that the model has a real value as an instrument of metabolic analysis, because it describes correctly, at least to a first approximation, the main characteristics of compartmentized energy metabolism of the cardiac cells.

DISCUSSION

Cellular and molecular biology of creatine kinases has undergone an impressive development over the last two decades; a detailed description of these systems, including that for the evolutionary tree of different isoenzymes, has already been given in numerous review articles and books (Wallimann et al., 1992; Koretsky, 1995; Saks and Ventura-Clapier, 1994; Saks et al., 1975, 1994, 1995, 1996; Soboll et al., 1992, 1994; Jacobus and Saks, 1982). At the same time, these developments have not yet influenced the metabolic analyses of the cardiac cell: practically all calculations in muscle metabolism are based on the simple equation of creatine kinase reaction equilibrium, ignoring the existence of compartmentalized creatine kinase isoenzymes. And this

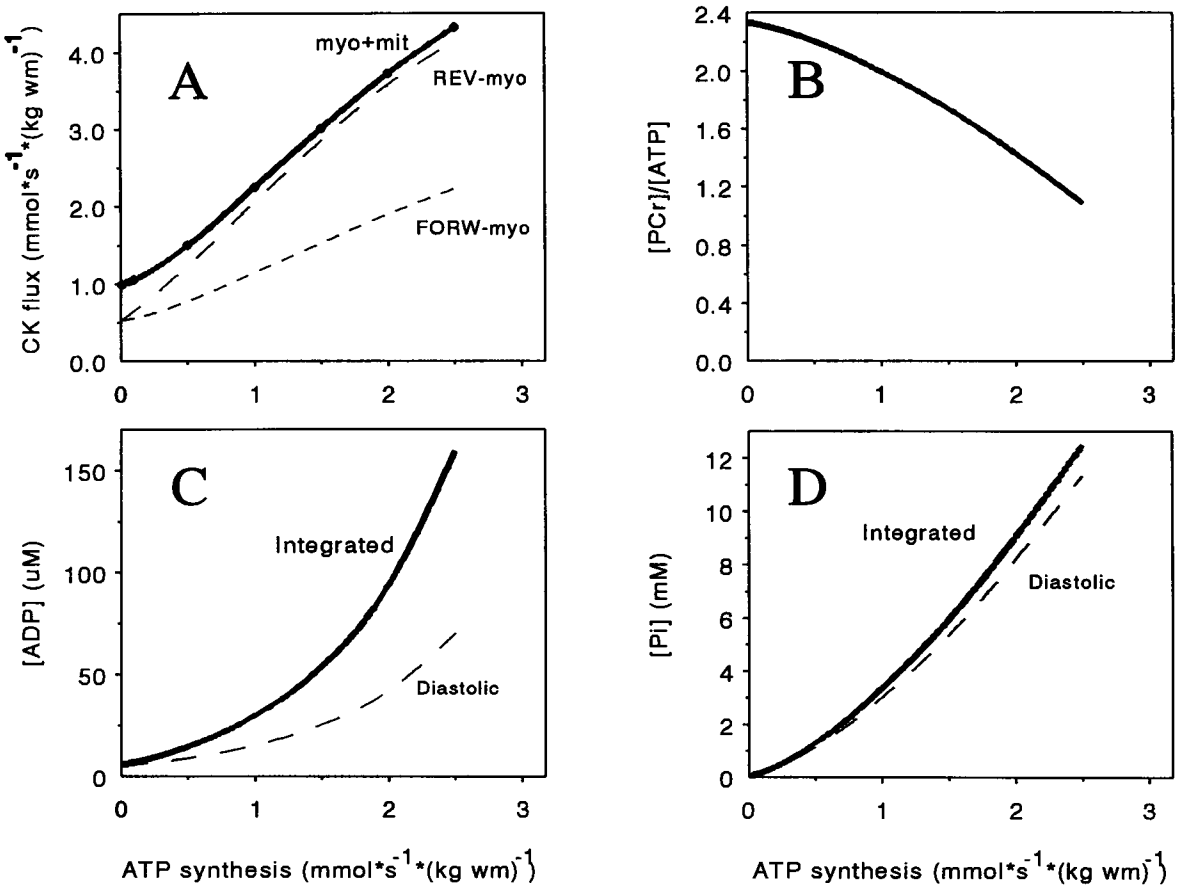

FIGURE 14 Unidirectional averaged steady-state fluxes through cellular creatine kinases (*A*) and myoplasmic metabolite levels (*B–D*) at different simulated workloads of the heart. Different workloads at a constant heart rate of 333 beats/min were modeled by taking the values of ATP hydrolysis in myofibrils (ATP_h in Table 1) to be 0.0018, 0.018, 0.09, 0.18, 0.27, 0.36, and 0.44 mmol × $beat^{-1}$ × (kg wet mass)$^{-1}$ in each separate simulation. Calculations were made for the complete system with diffusion restrictions as in Fig. 4. The values of all unidirectional fluxes (*A*), ADP (*C*), and P_i (*D*) concentrations were integrated throughout the cardiac cycle and cytoplasmic diffusion pathway (see Fig. 1) to obtain average data for comparison with those of the in vitro ^{31}P-NMR measurements. (*A*) Workload dependencies of unidirectional mean steady-state fluxes through CK_{myo} plus CK_{mit} (myo + mit, *thick line*) and CK_{myo} in the reverse (Rev-myo, *dashed thin line*) and forward (FORW-myo, *dotted thin line*) directions. The mean total unidirectional fluxes through CK_{myo} plus CK_{mit} are equal in the two directions. Therefore the differences between thick and thin lines indicate the contribution of CK_{mit} in unidirectional mean fluxes in the forward and reverse directions. The inequality of forward and reverse mean unidirectional fluxes catalyzed by particular creatine kinase isoforms again indicates their steady-state displacement from equilibrium. (*B*) Workload dependence of diastolic PCr/ATP ratios in the myofibrillar core. (*C* and *D*) Workload dependencies of mean ADP and P_i concentrations (integrated, *thick lines*), respectively, are compared with their diastolic levels in the myofibrillar core (diastolic, *dashed thin lines*).

simplified approach has been shown to be not very successful in explaining many phenomena related to respiration regulation (see Saks et al., 1995, for a review).

The aim of this work is to give the first mathematical description of the complete system of compartmentalized energy metabolism in the heart. This includes mitochondrial ATP synthase, mitochondrial isoenzyme of creatine kinase functionally coupled to oxidative phosphorylation via the adenine nucleotide translocase, myoplasmic creatine kinase, actomyosin ATPase, and diffusional exchange of metabolites between different compartments of the cell. We have mathematically modeled the most general scheme of the compartmentalized energy metabolism in cardiac cells on the basis of existing experimental data. For simplicity, we have made several assumptions regarding the properties of the system studied. The mathematical model given in this work, therefore, most probably describes the main, general features of the system. One of the very important characteristics of the model is that all parameters are experimentally determined and published earlier, except intracellular ADP concentration, which is calculated by model. It describes well the experimental data obtained with isolated heart mitochondria under precisely defined and controlled conditions (see Fig. 3). The assumptions made in the model concern the description of the coupling between mitochondrial creatine kinase and adenine nucleotide translocase, and the role of the latter in the regulation of metabolic fluxes. We have assumed that translocase functions in a rapid equilibrium mode using the most simple concept of Wilson, Erecinska, and Hassinen (Hassinen, 1986). Furthermore, we have assumed that ANT supplies ATP from mitochondria to the microcompartment between ANT and CK_{mit} in ex-

change with ADP from the intermembrane space. ADP in the intermembrane space is produced by mitochondrial creatine kinase according to the complete kinetic equation of the reaction, and comes from the cytoplasm by diffusion via the porin pores in the outer mitochondrial membrane, the permeability of which may be variable. Thus the model includes coupling of the ATP flux from mitochondria with PCr production. But it does not include the reverse process, direct coupling of ADP flux from CK_{mit} with its transport by ANT back into mitochondria for oxidative phosphorylation. This process was modeled by using a probability approach and precise kinetics of ANT in our previous works (Aliev and Saks, 1993, 1994) and shown to be important for the control of respiration by mitochondrial creatine kinase (Koretsky, 1995; Saks et al., 1996). This precise model could be introduced into the general one described in the present study for detailed analysis of respiration regulation, but it was omitted in this work because of its complexity and replaced by a simpler model of "loose" coupling of the reverse fluxes via ADP concentration in the intermembrane space. Furthermore, the distribution of creatine kinase in the myofibrillar space was taken to be homogeneous, and the binding of CK_{myo} to myofibrillar structures was ignored for the sake of simplicity of calculation. We also did not include other reactions, especially that of adenylate kinase, which modifies the concentration of ADP in the real system. This simplification may be justified, because Goldberger's group has shown that in aerobic muscles energy flux via the adenylate kinase system is minimal (Zeleznikar et al., 1995).

When applied to the analysis of the time-averaged values of metabolic parameters as a function of the workload, the model gives good agreement with the experimental results for the rates of mitochondrial phosphocreatine production and total creatine kinase flux as a function of ATP synthesis (Zahler et al., 1987; Perry et al., 1988; Zahler and Ingwall, 1992). This means that the coupling between oxidative phosphorylation and the mitochondrial creatine kinase reaction is adequately described by the model. However, the lack of description of functional coupling between actomyosin ATPase and myofibrillar creatine kinase (Ventura-Clapier et al., 1994) and reverse coupling in mitochondria may be the reason why the model yields a rather strong decrease in the PCr/ATP ratio and a correspondingly rapid elevation of phosphate level at increased workload. Moreover, the possibility of the vectorial ligand transduction for feedback regulation of respiration (Saks et al., 1994) has not yet been accounted for in this model. These are the perspectives that indicate the need for further development of the model.

The permeabilized cell technique has shown that, in contrast to isolated mitochondria in vitro, which have an apparent K_m for ADP equal to 10–20 μM, in cardiac, red skeletal muscle, and liver cells, the mitochondrial apparent K_m value for this substrate is increased by an order of magnitude to 300 μM (Saks and Ventura-Clapier, 1994; Saks et al., 1994, 1995, 1996). However, the apparent K_m for ADP is decreased after the rupture of the mitochondrial outer membrane in hypoosmotic medium, or by trypsin treatment (Saks et al., 1995). This shows that outer mitochondrial membrane permeability is controlled by some cytoplasmic protein, and we have hypothesized that this protein may take a part in vectorial ligand transduction system (Saks et al., 1995). This permeability has been shown to be increased in energy-deficient states and in transgenic mice without myoplasmic creatine kinase (Veksler et al., 1995; Clark et al., 1994). The influence of this low permeability of mitochondrial outer membrane for ADP in vivo and its adaptive changes were studied theoretically in this work.

An important property of the model is that it allows the calculation of compartmentalized fluxes (see Fig. 6) in cardiomyocytes related to functioning of the creatine kinases in mitochondria and cytoplasmic space (myofibrils). Some very interesting conclusions can be drawn from this analysis.

First, in mitochondria and even in cytoplasm, the creatine kinase isoenzymes are functioning rather far from the equilibrium in the steady state for the major part of the cardiac cycle (see Figs. 6, 8, and 10). It must be noted that the enzyme activities used in the model were those found experimentally, with the creatine kinase maximum activity in the cytoplasm (in the direction of ATP production) exceeding the rate of ATP synthase by an order of magnitude (see Table 1). This appears to be insufficient to establish equilibrium when the steady-state fluxes are elevated because of a high workload. Consequently, the assumption of the equilibrium usually accepted for creatine kinase in the literature and used to calculate ADP concentrations is at best a very rough approximation under these conditions. This assumption may be valid for resting muscle (Veech et al., 1979; Wiseman and Kushmerick, 1995), but increasing workload and energy fluxes very significantly shift the creatine kinase system out of equilibrium. This conclusion is in agreement with the results of theoretical analysis of the energy metabolism performed by Jurgen Daut in 1987 (Daut, 1987), who introduced the concept of a "metastable system" (meaning that the system is not at thermodynamic equilibrium, but represents a stable configuration in a steady state, and this may lead to questioning of the validity of the use of the creatine kinase equilibrium equation for calculation of ADP concentrations under these conditions). Usually support for the concept of creatine kinase equilibrium is found in NMR experiments, which have shown equality of the forward and reverse creatine kinase flux rate constants; however, this equality exists in any steady state of a complete system (Saks et al., 1994).

Second, among metabolic changes during the cardiac cycle, the levels of ATP and PCr change nonsignificantly because of matched fluxes in different compartments, in accordance with many experimental data (Wan et al., 1993; Balaban, 1990; Sievers et al., 1983; Wikman-Coffelt et al., 1983). Very significant changes are observed only for ADP, and its cytoplasmic concentration depends both on the func-

tioning of creatine kinase isoenzymes and regulation of the porin channels in the outer mitochondrial membrane.

In the whole system, with all creatine kinase isoenzymes in place, low permeability of the outer mitochondrial membrane for adenine nucleotides has one clear, rather positive effect: it stabilizes the rate of mitochondrial production of PCr, which becomes almost the exclusive energy exporter from mitochondria (Figs. 6 and 7). Thus the low mitochondrial outer membrane permeability for adenine nucleotides strongly compartmentalizes them in mitochondria and stabilizes mitochondrial reactions of energy production. Studies of the model behavior carried out in this work showed that most probably, the existence of the separate mitochondrial creatine kinase isoenzyme in cardiac and other types of cells is directly related to this limited, controlled permeability of the outer mitochondrial membrane for adenine nucleotides and the strong compartmentalization of their turnover in the intermembrane space. In this case, the mitochondrial creatine kinase becomes essential, and its inhibition reduces steady-state levels of PCr by ~3 times (see Table 2). Recently we have shown that the coupled CK_{mit}-ANT system in mitochondria has increased control properties (Saks et al., 1996). However, it is still not clear which protein controls mitochondrial outer membrane permeability and precisely for which propose. Most probably this is related to fine regulation and vectorial signal conduction (for this hypothesis see Saks et al., 1995, 1996).

Low permeability of the outer mitochondrial membrane becomes a negative factor, disturbing cellular energy metabolism in the case of "knock-out" of any of the creatine kinase isoenzymes. Without restrictions of the adenine nucleotide diffusion into mitochondria, the different creatine kinase isoenzymes may to some degree replace each other in the cellular energy metabolism by taking over their function. For example, in the absence of myoplasmic creatine kinase, CK_{mit} catalyzes the PCr utilization at the peak of the contraction phase (Fig. 8). This is exactly what was observed by van Deursen et al. (1993, 1994b) in transgenic mice—they observed both PCr production and utilization in muscles of mice lacking myoplasmic creatine kinase. This "takeover" is more significant if the permeability of the mitochondrial outer membrane is increased, and this indeed was observed by Veksler et al. (1995) as an adaptive change in these animals. Nevertheless, the system does not achieve the efficiency of the complete system in maintaining low cytoplasmic ADP levels (see Table 2). That may be a reason for the decreased burst contractile activity observed in experiments (van Deursen et al., 1993, 1994a,b).

Whereas the absence of myoplasmic creatine kinase results mostly in elevation of the ADP levels in cytoplasm, "knock-out" of CK_{mit} results in decreased PCr production that is now catalyzed by CK_{myo} because of its significant shift from equilibrium (Fig. 10). This is clearly the case when it seems to be impossible to satisfy the temptation to use a simple equilibrium equation for creatine kinase—the equilibrium never exists, according to our calculations. In the systolic phase, myoplasmic creatine kinase, as usual, rephosphorylates ADP, depending on the availability of PCr, but in the diastolic phase it produces PCr, driven by mitochondrial synthesis of ATP, and, correspondingly, removes ADP—the steady state rates of these processes become close (Fig. 10). Without coupling in mitochondria, these processes become less effective and the PCr level decreases, especially if there are restrictions of adenine nucleotide diffusion across mitochondrial membrane (Table 2). This is similar to coupling of PCr production to glycolysis, and cardiac muscle in a CK_{mit}-lacking animal may have some similarities to glycolytic muscles with respect to slow PCr production and rapid utilization. On the basis of our calculations we may predict that another useful adaptive change in this case could be a decrease in restriction of the diffusion of adenine nucleotides across the outer mitochondrial membrane (see Fig. 10). Whether this mechanism is used by nature, or is substituted by other effective adaptive mechanisms such as the activation of the adenylate kinase pathway (Zeleznikar et al., 1995), may be found out in further experiments.

Experimentally, this situation has been modeled by van Deursen et al. (1994a) by inducing Cr and PCr deficiency in CK_{myo}-lacking transgenic mice, and the results show, in concord with our predictions, deterioration of muscle function, most probably due to accumulation of ADP (see Table 2), which slows down cross-bridge detachment and the contraction cycle (Ventura-Clapier et al., 1994).

Thus, in general, predictions from the use of our model described in this work are in qualitative accordance with many recent experimental data. However, a more complete mathematical model of cellular energy metabolism probably needs to incorporate several important additional systems, such as adenylate kinase, close functional coupling and compartmentalization of creatine kinase in myofibrils, glycolytic ATP production, and, finally, vectorial ligand conduction as a possible feedback signal (Saks et al., 1994). All of this is possible on the basis of the model presented here. These are questions for further work, depending on the task, available calculation time, and degree of complexity acceptable for real use of the model.

The authors thank Dr. Vladimir Veksler for critical discussion of this paper and Dr. Ernest Boehm for correcting the English.

This work was supported by grants from the International Association for the promotion of co-operation with scientists from the formerly Soviet Union (INTAS 94-4738), Estonian Science Foundation (1938), and in part by the Russian Foundation for Basic Research (97-04-49554).

REFERENCES

Aliev, M. K., and V. A. Saks. 1993. Quantitative analysis of the phosphocreatine shuttle. I. A probability approach to the description of phosphocreatine production in the coupled creatine kinase-ATP/ADP translocase-oxidative phosphorylation reactions in heart mitochondria. *Biochim. Biophys. Acta.* 1143:291–300.

Aliev, M. K., and V. A. Saks. 1994. Mathematical modeling of intracellular transport processes and the creatine kinase systems: a probability approach. *Mol. Cell. Biochem.* 133/134:333–346.

Anversa, P., G. Olivetti, M. Melissari, and A. V. Loud. 1979. Morphometric study of myocardial hypertrophy induced by abdominal aortic stenosis. *Lab. Invest.* 40:341–349.

Balaban, R. S. 1990. Regulation of mitochondrial oxidative phosphorylation in mammalian cells. *Am. J. Physiol.* 258:C377–C389.

Bittl, J. A., J. DeLayre, and J. S. Ingwall. 1987. Rate equation for creatine kinase predicts the in vivo reaction velocity: ^{31}P NMR surface coil studies in brain, heart, and skeletal muscle of the living rat. *Biochemistry.* 26:6083–6090.

Clark, J. F., Z. A. Khuchua, A. V. Kuznetsov, E. V. Vassilieva, E. Boehm, G. K. Radda, and V. A. Saks. 1994. Actions of the creatine analogue β-guanidinopropionic acid on rat heart mitochondria. *Biochem. J.* 300: 211–216.

Cleland, W. W. 1967. Enzyme kinetics. *Annu. Rev. Biochem.* 36:77–112.

Crank, J. 1975. The Mathematics of Diffusion, 2nd Ed. Clarendon Press, Oxford. 137–144.

Daut, J. 1987. The living cell as energy-transducing machine. A minimal model of myocardial energy metabolism. *Biochim. Biophys. Acta.* 895: 41–62.

Ebert, K., and H. Ederer. 1985. Computeranwendungen in der Chemie, Section 9.8. VCH Verlagsgesellschaft mbH, Weinheim, Germany. 251–257.

Elzinga, G., and W. J. van der Laarse. 1990. MVO_2max of the heart cannot be determined from uncoupled myocytes. *Basic Res. Cardiol.* 85: 315–317.

Fossel, E., and H. Hoefeler. 1987. A synthetic functional metabolic compartment. The role of propinquity in a linked pair of immobilised enzymes. *Eur. J. Biochem.* 170:165–171.

Giesen, J., and H. Kammermeier. 1980. Relationship of phosphorylation potential and oxygen consumption in isolated perfused rat heart. *J. Mol. Cell. Cardiol.* 12:891–907.

Gyulai, L., Z. Roth, J. S. Leigh, and B. Chance. 1985. Bioenergetic studies of mitochondrial oxidative phosphorylation using ^{31}Phosphorus NMR. *J. Biol. Chem.* 260:3947–3954.

Hassinen, I. E. 1986. Mitochondrial respiratory control in myocardium. *Biochim. Biophys. Acta.* 853:135–151.

Holian, A., C. S. Owen, and D. F. Wilson. 1977. Control of respiration in isolated mitochondria: quantitative evaluation of the dependence of respiratory rates on [ATP], [ADP], and [P_i]. *Arch. Biochem. Biophys.* 181:164–171.

Jacobus, W. E., and V. A. Saks. 1982. Creatine kinase of heart mitochondria: changes in its kinetic properties induced by coupling to oxidative phosphorylation. *Arch. Biochem. Biophys.* 219:167–178.

Kenyon, G. L., and G. H. Reed. 1983. Creatine kinase: structure-activity relationships. *Adv. Enzymol.* 54:367–426.

Klingenberg, M., and H. Rottenberg. 1977. Relation between the gradient of the ATP/ADP ratio and the membrane potential across the mitochondrial membrane. *Eur. J. Biochem.* 73:125–130.

Koretsky, A. P. 1995. Insights into cellular energy metabolism from transgenic mice. *Physiol. Rev.* 75:667–688.

Kupriyanov, V. V., A. Ya. Steinschneider, E. K. Ruuge, V. I. Kapelko, M. Yu. Zueva, V. L. Lakomkin, V. N. Smirnov, and V. A. Saks. 1984. Regulation of energy flux through the creatine kinase reaction in vitro and in perfused rat heart. *Biochim. Biophys. Acta.* 805:319–331.

Meyer, R. A., H. L. Sweeney, and M. J. Kushmerick. 1984. A simple analysis of the "phosphocreatine shuttle." *Am. J. Physiol.* 246: C365–C377.

Perry, S. P., J. McAuliffe, J. A. Balschi, P. R. Hickey, and J. S. Ingwall. 1988. Velocity of the creatine kinase reaction in the neonatal rabbit heart: role of mitochondrial creatine kinase. *Biochemistry.* 27: 2165–2172.

Saks, V. A. 1980. Creatine kinase isoenzymes and the control of cardiac contraction. *In* Heart Creatine Kinase. The Integration of Isozymes for Energy Distribution. W. E. Jacobus and J. S. Ingwall, editors. Williams and Wilkins, Baltimore, MD. 109–126.

Saks, V. A., and M. K. Aliev. 1996. Is there creatine kinase equilibrium in working heart cells? *Biochem. Biophys. Res. Commun.* 227:360–367.

Saks, V. A., G. B. Chernousova, D. E. Gukovsky, V. N. Smirnov, and E. I. Chazov. 1975. Studies of energy transport in heart cells. Mitochondrial isoenzyme of creatine kinase: kinetic properties and regulatory action of Mg^{2+} ions. *Eur. J. Biochem.* 57:273–290.

Saks, V. A., G. V. Chernousova, R. Vetter, V. N. Smirnov, and E. I. Chazov. 1976. Kinetic properties and functional role of particulate MM-isoenzyme of creatine phosphokinase bound to heart muscle myofibrils. *FEBS Lett.* 62:293–296.

Saks, V. A., Z. A. Khuchua, E. V. Vasilyeva, O. Yu. Belikova, and A. V. Kuznetsov. 1994. Metabolic compartmentation and substrate channeling in muscle cells. Role of coupled creatine kinases in in vivo regulation of cellular respiration—a synthesis. *Mol. Cell. Biochem.* 133/134:155–192.

Saks, V. A., A. V. Kuznetsov, Z. A. Khuchua, E. V. Vasilieva, Y. O. Belikova, T. Kesvatera, and T. Tiivel. 1995. Control of cellular respiration in vivo by mitochondrial outer membrane and by creatine kinase. A new speculative hypothesis: involvement of mitochondrial-cytoskeletal interactions. *J. Mol. Cell. Cardiol.* 27:625–645.

Saks, V. A., A. V. Kuznetsov, V. V. Kupriyanov, M. V. Miceli, and W. E. Jacobus. 1985. Creatine kinase of rat heart mitochondria. The demonstration of functional coupling to oxidative phosphorylation in an inner membrane-matrix preparation. *J. Biol. Chem.* 260:7757–7764.

Saks, V. A., and R. Ventura-Clapier, editors. 1994. Cellular Bioenergetics: Role of Coupled Creatine Kinases. Kluwer Academic Publishers, Dordrecht, Boston, London. 1–346.

Saks, V. A., R. Ventura-Clapier, and M. K. Aliev. 1996. Metabolic control and metabolic capacity: two aspects of creatine kinase functioning in the cells. *Biochim. Biophys. Acta.* 1274:81–96.

Saks, V. A., R. Ventura-Clapier, Z. A. Huchua, A. N. Preobrazhensky, and I. V. Emelin. 1984. Creatine kinase in regulation of heart function and metabolism. I. Further evidence for compartmentation of adenine nucleotides in cardiac myofibrillar and sarcolemmal coupled ATPase-creatine kinase systems. *Biochim. Biophys. Acta.* 803:254–264.

Smith, H. E., and E. Page. 1976. Morphometry of rat heart mitochondrial subcompartments and membranes: application to myocardial atrophy after hypophysectomy. *J. Ultrastruct. Res.* 55:31–41.

Soboll, S., A. Conrad, and S. Hebisch. 1994. Influence of mitochondrial creatine kinase on the mitochondrial/extramitochondrial distribution of high energy phosphates in muscle tissue: evidence for a leak in the creatine shuttle. *Mol. Cell. Biochem.* 133/134:105–113.

Soboll, S., A. Conrad, M. Keller, and S. Hebish. 1992. The role of the mitochondrial creatine kinase system for myocardial functioning during ischemia and reperfusion. *Biochim. Biophys. Acta.* 1100:27–32.

Sievers, R., W. W. Parmley, T. James, and J. Wikman-Coffelt. 1983. Energy levels at systole vs. diastole in normal hamster hearts vs. myopathic hamster hearts. *Circ. Res.* 53:759–766.

Steeghs, K., F. Oerlemans, and B. Wieringa. 1995. Mice deficient in ubiquitous mitochondrial creatine kinase are viable and fertile. *Biochim. Biophys. Acta.* 1230:130–138.

van Deursen, J., A. Heerschap, F. Oerlemans, W. Ruitenbeek, P. Jap, H. Ter Laak, and B. Wieringa. 1993. Skeletal muscles of mice deficient in muscle creatine kinase lack burst activity. *Cell.* 74:621–631.

van Deursen, J., P. Jap, A. Heerschap, H. Ter Laak, W. Ruitenbeek, and B. Wieringa. 1994a. Effects of the creatine analogue on skeletal muscle of mice deficient in muscle cretine kinase. *Biochim. Biophys. Acta.* 1185: 327–335.

van Deursen, J., W. Ruitenbeek, A. Heerschap, P. Jap, H. Ter Laak, and B. Wieringa. 1994b. Creatine kinase (CK) in skeletal muscle energy metabolism: a study of mouse mutants with graded reduction in muscle CK expression. *Proc. Natl. Acad. Sci. USA.* 91:9091–9095.

Veech, R. L., J. W. R. Lawson, N. W. Cornell, and H. A. Krebs. 1979. Cytosolic phosphorylation potential. *J. Biol. Chem.* 254:6538–6547.

Veksler, V. I., A. V. Kuznetsov, K. Anflous, P. Mateo, J. van Deursen, B. Wieringa, and R. Ventura-Clapier. 1995. Muscle creatine kinase deficient mice. II. Cardiac and skeletal muscle exhibit tissue-specific adaptation of the mitochondrial function. *J. Biol. Chem.* 270: 19921–19929.

Ventura-Clapier, R., V. A. Saks, G. Vassort, C. Lauer, and G. V. Elizarova.

1987. Reversible MM-creatine kinase binding to cardiac myofibrils. *Am. J. Physiol.* 253:C444–C455.

Ventura-Clapier, R., V. I. Veksler, and J. A. Hoerter. 1994. Myofibrillar creatine kinase and cardiac contraction. *Mol. Cell. Biochem.* 133/134: 125–144.

Wallimann, T., M. Wyss, D. Brdiczka, K. Nicolay, and H. Eppenberger. 1992. Intracellular compartmentation, structure and function of creatine kinase isoenzymes in tissues with high and fluctuating energy demands: the "phosphocreatine circuit" for cellular energy homeostasis. *Biochem. J.* 281:21–40.

Wan, B., C. Dounen, J. Duszynsky, G. Salama, T. C. Vary, and K. F. Lanoue. 1993. Effect of cardiac work on electrical potential gradient across mitochondrial membrane in perfused hearts. *Am. J. Physiol.* 265:H453–H460.

Wikman-Coffelt, J., R. Sievers, R. Coffelt, and W. W. Parmley. 1983. The cardiac cycle: regulation and energy oscillations. *Am. J. Physiol.* 245: H345–H362.

Williamson, J. R., G. Ford, J. Illingworth, and B. Safer. 1976. Coordination of citric acid activity with electron transport flux. *Circ. Res.* 38(Suppl. I):I39–I51.

Wiseman, R. W., and M. J. Kushmerick. 1995. Creatine kinase equilibration follows solution thermodynamics in skeletal muscle. *J. Biol. Chem.* 270:12428–12438.

Zahler, R., J. A. Bittl, and J. S. Ingwall. 1987. Analysis of compartmentation of ATP in skeletal and cardiac muscle using ^{31}P nuclear magnetic resonance saturation transfer. *Biophys. J.* 512:883–893.

Zahler, R., and J. S. Ingwall. 1992. Estimation of heart mitochondrial creatine kinase flux using magnetisation transfer NMR spectroscopy. *Am. J. Physiol.* 262:H1022–H1028.

Zeleznikar, R. J., P. P. Dzeja, and N. D. Goldberg. 1995. Adenylate kinase-catalysed phosphoryl transfer couples ATP utilization with its generation by glycolysis in intact muscle cells. *J. Biol. Chem.* 270: 7311–7319.